APPROVED FOR RELEASE: 2007/02/08: CIA-RDP82-00850R000300030023-0

JPRS L/9303

17 September 1980

USSR Report

SPACE

(FOUO 8/80)

FBIS FOREIGN BROADCAST INFORMATION SERVICE

APPROVED FOR RELEASE: 2007/02/08: CIA-RDP82-00850R000300030023-0

NOTE

JPRS publications contain information primarily from foreign newspapers, periodicals and books, but also from news agency transmissions and broadcasts. Materials from foreign-language sources are translated; those from English-language sources are transcribed or reprinted, with the original phrasing and other characteristics retained.

Headlines, editorial reports, and material enclosed in brackets [] are supplied by JPRS. Processing indicators such as [Text] or [Excerpt] in the first line of each item, or following the last line of a brief, indicate how the original information was processed. Where no processing indicator is given, the information was summarized or extracted.

Unfamiliar names rendered phonetically or transliterated are enclosed in parentheses. Words or names preceded by a question mark and enclosed in parentheses were not clear in the original but have been supplied as appropriate in context. Other unattributed parenthetical notes within the body of an item originate with the source. Times within items are as given by source.

The contents of this publication in no way represent the policies, views or attitudes of the U.S. Government.

For further information on report content call (703) 351-2938 (economic); 3468 (political, sociological, military); 2726 (life sciences); 2725 (physical sciences).

APPROVED FOR RELEASE: 2007/02/08: CIA-RDP82-00850R000300030023-0

JPRS L/9303

17 September 1980

USSR REPORT

SPACE

(FOUO 8/80)

CONTENTS

LIFE SCIENCES

SOYUZ-T SURVIVAL SUITS PICTURED

Paris AIR & COSMOS in French No 819, 28 Jun 80 pp 44, 56

[Article by S.B.: "'Soyuz-T', A New Generation Soviet Vehicle"]

[Excerpt] A new space suit, called a "survival suit," was used [on board Soyuz-T]. It protects cosmonauts in the case of acute cabin depressurization. This suit is lighter (two times lighter than that worn by Gagarin), more flexible, and can be put on rapidly. Thanks to a "transparent steel" visor, the cosmonaut's field of vision is greater. Even when the suit is inflated, the cosmonaut can, while wearing his gloves, wind his watch or pick up a needle.

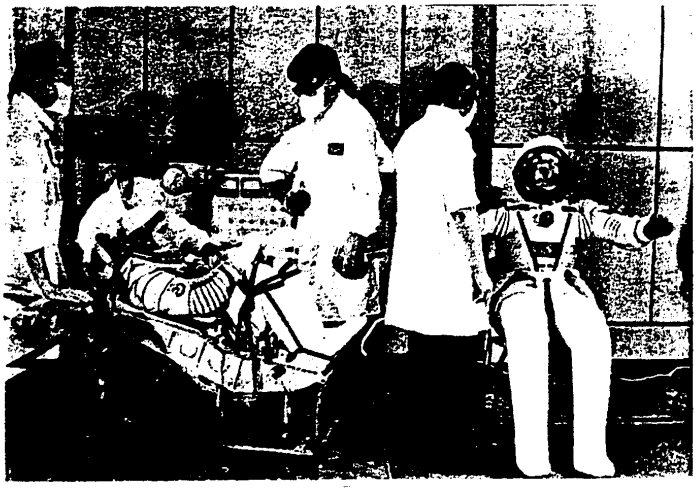

The Soyuz-T crew, Malyshev and Aksenov (left to right), wearing the new space "survival suit" which was flight tested for the first time.

[1853/11-P]

CSO: 1853

SPACE APPLICATIONS

UDC 629.19:551

TRAJECTORIES OF SPACE VEHICLES INTENDED FOR INVESTIGATION OF THE EARTH FROM SPACE

Moscow ISSLEDOVANIYE ZEMLI IZ KOSMOSA in Russian No 3, 1980 pp 91-97

[Article by Ye. L. Lukashevich, State Scientific Research and Production Center "Priroda"]

[Text] One of the important stages in investigating the earth from space is the collection aboard a space vehicle of information concerning the state of the atmosphere, lithosphere and hydrosphere of our planet. The realization of this stage involves, in particular, solving the problem of positioning the space vehicle in near-earth space in such a way as will allow an orderly scanning of the entire surface of the planet or a stipulated spherical zone in a relatively short time interval, taking into account a number of specific requirements and restrictions on the difference in scale of the collected information, on the periodicity of repeated observations of one and the same regions, on the illumination of the earth's surface, etc. We will examine the peculiarities of the trajectory of a space vehicle which will satisfy the most important of the enumerated requirements as well as methods for computing the nominal parameters of these trajectories.

A necessary and adequate condition for ensuring a full scanning of the earth's surface within the limits of the observed latitude zone is that the orbit belong to a class of quasigeosynchronous trajectories with such a relationship between the Draconian period of revolution of the space vehicle and the diurnal rotation of the earth in which the trajectory of the K-th revolution will pass in the neighborhood of the trajectory of the $(K - N_m)$-th revolution. In this case the number of revolutions N_m between two successive passes of the trajectory through the neighborhood of an arbitrary point on the surface is the "order" of the orbit and the number of days m in which the space vehicle makes N_m revolutions is the "multiplicity" of the orbit. The distance between the trajectories of the $(K - N_m)$-th and K-th revolutions is determined by the width of the zone of scanning of the on-board observation systems.

There are different algorithms for computing the nominal parameters of the quasigeosynchronous trajectories, differing from one another in the use of different intermediate orbits. However, all these algorithms are derived from an expression representing the mathematical writing of the principle of quasigeosynchronicity of motion:

$$\Delta L=2\pi m-\omega TN_m+\Delta\Omega_m, \tag{1}$$

where ΔL is the angular displacement of the flight trajectory in N_m revolutions, ω is the angular velocity of the earth's diurnal rotation, T is the Draconian period of revolution of the space vehicle, $\Delta\Omega_m$ is the change in longitude of the ascending node in m days. We can become familiar with a general case of computation of geosynchronous trajectories, constructed in Keplerian intermediate orbits, in such studies as [1]. Applicable to the problem of investigation of natural resources the algorithm for computing the altitude of a circular quasigeosynchronous perturbed Keplerian orbit was proposed in [2].

We note that in most cases the $\Delta\Omega_m$ and ΔL parameters are commensurable and therefore the choice of parameters and the evaluation of stability of quasigeosynchronous trajectories must be carried out with rigorous allowance for precession of the orbital plane, caused primarily by the influence of acentrality of the planetary gravitational field. In this connection it is desirable in the stage of ballistic planning of such trajectories to use models of the gravitational field taking into account the fundamental harmonics of the earth's gravitational potential. As such a model in [3] use was made of the gravitational field of three pairs of fixed centers with complexly conjugate masses situated on the z-axis of a geocentric equatorial coordinate system. According to the estimates cited in [4], such a model of the gravitational field makes it possible to take into account the perturbations caused by the influence of the totality of the first zonal harmonics of the earth's potential (to the eighth inclusive).

Now we will examine the procedure for computing the nominal parameters of quasigeosynchronous orbits based on the simplified algorithms in [3]. Expanding the T and $\Delta\Omega_m$ parameters in expression (1), after simple transformations it is easy to obtain an equation transcendental relative to the semimajor axis which with an accuracy to terms of the order of the square of the earth's flattening inclusive can be represented in the following form:

$$a_0^{3/2}=\frac{\sqrt{fM}}{\omega N_m}\left(m-\frac{\Delta L_0}{2\pi}-\frac{3}{2}\alpha\varepsilon_0^2N_m\right)\left[1+\frac{3}{2}\varepsilon_0^2\left(1-\frac{3}{2}s^2+e_0^2\alpha^2\right)\right], \tag{2}$$

where f is the gravitational constant, s and α are the sine and cosine of the angle of inclination, $\varepsilon_0 = R\sqrt{-I_2}/a_0(1 - e_0^2)$, M and R are the mass and mean equatorial radius of the earth, I_2 is a coefficient on the second zonal harmonic of the earth's gravitational potential. This expression makes it possible to use the iteration method to determine the nominal

semimajor axis a_0 of a quasigeosynchronous orbit using the stipulated values of the initial eccentricity e_0, inclination i, initial displacement of the trajectory ΔL_0 and the range of the working altitudes $[h_{min}, h_{max}]$, which characterizes the order N_m and multiplicity m of the orbit.

We note that from the condition of obtaining information with minimum scale scatters it is preferable to have circular orbits for the considered class of space vehicles. However, as a result of the peculiarities of putting a space vehicle into an orbit with the mean altitude $h \in [h_{min}, h_{max}]$ as a rule one obtains a near-circular trajectory with a certain e0 value. The inclination of the orbital plane to the equatorial plane is selected from the condition $i = \varphi_{max}$, where φ_{max} is the maximum latitude of the subsatellite point. Finally, the displacement of the trajectory ΔL_0 is chosen so that it is commensurable with the width l of the scanning zone, taking into account the necessary transverse overlap of adjacent zones at the stipulated latitude φ. It must be remembered that sign ΔL_0 determines the direction of the displacement: with $\Delta L_0 > 0$ the trajectory is displaced to the east; with $\Delta L_0 < 0$ -- to the west.

The following sequence is proposed for computing the semimajor axis with the use of equation (2).

1. Taking into account the possibility of putting a space vehicle into a working orbit, the width of the scanning zone when making observations from a stipulated range of working altitudes, the lateral overlap of the scanning zones at a stipulated latitude and the maximum latitude of the territory subject to observation, we will determine the elements $e_0, |\Delta L_0|$, i. In this case it is possible to use the obvious expression

$$|\Delta L_0| = (l^* - \Delta l_0^*)/R\cos\varphi, \tag{3}$$

where $l^* = l(s^2 - \alpha^2 tg^2\varphi)^{-1/2}$ is the extent of the scanning zone along the parallel at the latitude φ, Δl_0^* is the initial lateral overlap of the scanning zones at the latitude φ.

2. Using the simplified expression following from condition (1)

$$\Delta L \approx 2\pi\left[m - \frac{\omega}{\sqrt{fM}}\left(\frac{h_{min}+h_{max}}{2}\right)^{3/2} N_m\right], \tag{4}$$

we will determine the multiplicity and order of the orbit, as well as sign ΔL. It must be remembered that m and N_m are whole numbers related by the expressions: $N_m = 16m - n$, where $n = 1, 2, 3, \ldots$, when m and n are not multiple numbers and $N_m/n - 1$ for a case of multiple m and n. The sought-for parameters must ensure $\min|F(N_m, m, \text{sign } \Delta L)|$, where F is the difference of the right and left sides of the approximate equation (4). Good results are obtained from a graphic solution of equation (4) with use of the preconstructed regularities $\Delta L = \Delta L(h)$, where $h = (h_{min} + h_{max})/2$, for some m and N_m values. For example, in the range of working altitudes

200-1400 km it is sufficient for this to have orbits having the following order characteristics: $N_1 = 16$, $N_3 = 47$, $N_2 = 31$, $N_3 = 46$, $N_1 = 15$, $N_3 = 44$, $N_2 = 29$, $N_3 = 43$, $N_1 = 14$, $N_3 = 41$, $N2 = 27$, $N_3 = 40$, $N_1 = 13$, $N_3 = 38$, $N_2 = 25$.

3. Assuming that in a zero approximation $a_0^{(0)} = R + (h_{max} + h_{min})/2$ and substituting the determined e_0, m, N_m, ΔL_0 values and the known parameters ε_0, s, α into equation (2), we will compute the semimajor axis $a_0^{(1)}$ in the first approximation.

4. Refining the ε_0 parameter with allowance for $a_0^{(1)}$, from expression (2) we obtain a second approximation of the semimajor axis $a_0^{(2)}$. Then, continuing the iteration process, it is possible to determine the a_0 value with any stipulated accuracy.

It can happen that orbital eccentricity cannot be ascertained prior to the determination of a_0. Then it is necessary that the successive approximation in computation of the semimajor axis begin with the assumption that in the zero approximation $e_0^{(0)} = 0$. The radius r_{cir} of the circular orbit obtained under this condition from equation (2) is assumed to be the semimajor axis and the eccentricity is then determined from the minimum and maximum altitudes which the carrier-rocket can ensure when putting a space vehicle into an orbit with $a_0 = r_{cr}$. The eccentricities $e_0^{(1)}$ determined in such a way are again introduced into expression (2) and we will repeat the entire procedure of computations for the purpose of refining a_0.

It is easy to note that by extending the region of quasigeosynchronous trajectories to multiple orbits with $m > 1$, with virtually no limit we will broaden the range of altitudes applicable for selecting the working orbits of space vehicles of the considered class. The sequence for scanning zones on the earth's surface from orbits of different multiplicity is different. It can be shown that there is the following regularity making it possible to estimate the total number of revolutions N_Σ necessary for total scanning of the observed surface:

$$N_\Sigma = [\gamma/m]N_m + (\gamma - m[\gamma/m])([\gamma/m]+1) - 1,$$

where $\gamma = T_0\omega/\Delta L_0$ is the number of scanning bands in each interval between revolutions, T_0 is the initial value of the period of revolution. By insignificantly changing the ΔL_0 value it can be achieved that γ is a whole number.

One of the interesting peculiarities of use of multiple orbits is the possibility of selecting different observation schemes when working with one and the same altitude or with near-lying altitudes. For example, a space vehicle moving at an altitude $\sim$390 km and having a scanning zone of about 5° can have two order characteristics of a circular polar orbit: $N_2 = 31$ with displacement of the flight trajectory in an easterly direction and $N_3 = 47$ with displacement of the trajectory in a westerly direction.

Now we will examine the problem of illumination of features observed at the planetary surface. This problem is one of the most important in the planning and organization of space surveys with the use of photographic and television remote sounding systems.

The illumination of features situated on the earth's surface and in the neighborhood of the flight trajectory is determined by the relative orientation of the orbital plane and the plane passing through the mean terminator line. The principal factor governing precession of the orbital plane is acentrality of the gravitational field. The secular component of this precession in m days with an accuracy to the square of the earth's flattening can be represented in the form

$$\Delta\Omega_m = -3\pi\alpha\varepsilon^2 N_m. \tag{5}$$

The plane of the terminator also rotates as a result of the annual revolution of the earth around the sun. If $\alpha \geqslant 0$ ($i \leqslant 90°$), both planes rotate in opposite directions and the branch of the flight trajectory on which the survey occurs periodically emerges from the region of solar altitudes admissible for space photography. If the period of active operation of the space vehicle does not exceed a month, the choice of the corresponding moment of the launching can be achieved by continuous observation of the earth with satisfactory illumination of its surface. However, if the period of active operation of the space vehicle is more than a month, with emergence of the working branch of the trajectory from the region with satisfactory illumination a pause appears in the operation of the space vehicle and the continuity of observation is disrupted. With $\alpha < 0$ ($i > 90°$) both the orbital plane and the plane of the terminator rotate in one and the same direction. Thus, it is possible to select such an inclination that the angular velocities of rotation of both planes will be equal and heliosynchronous and the orbit will be solar-synchronous. The principal advantage of space vehicle motion in such an orbit is a constancy of the local time of transit over regions situated at one and the same latitude. In addition, solar-synchronous orbits have a number of merits favoring an increase in the effectiveness of long-term observation of the planetary surface with the use of space technology.

The methods for computing the elements of a solar-synchronous orbit, especially with the use of Keplerian intermediate orbits, are well known. Here we will use a somewhat different approach to choice of orbital parameters, and in particular, inclination, based on the fact that a solar-synchronous trajectory must at the same time be quasigeosynchronous.

Under the condition that in the course of one tropical year T_γ the orbital precession is a value 2π, from expression (5), with an accuracy to terms of the order of the square of planetary flattening inclusive, we obtain the following equation transcendental relative to the nominal a_0 value

$$a_0'' = -\frac{3\alpha e_0^2\sqrt{fM}}{2n^*}\left[1+\frac{3}{2}e_0^2\left(1-\frac{3}{2}s^2+e_0^2\alpha^2\right)\right], \tag{6}$$

where $n^* = 2\pi/T\gamma$ is the mean angular velocity of the earth's motion around the sun. By comparing expressions (2) and (6) it is easy to derive a simple expression for determining the α value of a solar-synchronous quasigeosynchronous orbit in dependence on ΔL_0, N_m and m:

$$\alpha = -\frac{2}{3\varepsilon_0^2 N_m}\cdot\frac{2\pi m-\Delta L_0}{\omega T_\gamma - 2\pi}. \tag{7}$$

For more rigorous computation of the orbital parameters it is necessary to have a joint solution of equations (2) and (6) by the iterations method. As a first approximation of α it is possible to use a value computed using formula (7).

Now we will turn to the problem of the stability of a quasigeosynchronous orbit and the maintenance of its parameters, in particular, the semimajor axis, in an admissible range. The principal perturbing factor exerting an influence on the secular change in a_0 and e_0 is the earth's atmosphere. An evaluation of these changes in the ballistic planning stage for orbits with a small eccentricity can be carried out using a static atmosphere using the formulas in [5]:

$$\Delta a = -4\pi c a_0^2 \rho_\pi \exp(-\nu)(1+\nu^2/4),$$
$$\Delta e = -2\pi c a_0 (1-e_0^2)\rho_\pi \exp(-\nu)\nu(1+\nu^2/8),$$

where Δa and Δe are the secular perturbation of the semimajor axis and eccentricity during one revolution of the space vehicle; c is the ballistic coefficient; ρ_π is atmospheric density at orbital perigee; $\nu = a_0 e_0/H$, H is the height of the homogeneous atmosphere. In d days the semimajor axis changes by the value $\Delta a d N_m$, which leads to a change in the Draconian period of revolution and in the last analysis to a noncorrespondence between the displacement of the trajectory ΔL and the width l of the scanning zone. The period of revolution on the d-th day of flight with an accuracy to values of the order ε^2 inclusive is determined using the formula

$$T = \frac{2\pi\sqrt{a^3}}{\sqrt{fM}}\left[1-\frac{3}{2}e^2\left(1-\frac{3}{2}s^2+e^2\alpha^2\right)\right],$$

where $a = a_0 + \Delta a d N_m$, $e = e_0 + \Delta e d N_m$. Disruptions in the conditions for lateral overlaps of adjacent scanning zones are evaluated using expressions (1) and (3). The latter makes it possible, on the basis of the ΔL value, changing after d days of flight, to determine the new Δl^* value at the stipulated latitude φ. For orbits with a westerly displacement of the flight trajectories this disruption will be expressed in the form of a progressive slipping of the zones relative to one another and this can lead to an incomplete scanning of the inter-revolution intervals if the number of

days D of active operation of the space vehicle is limited: $D \leqslant L/\Delta L_0$, where L is the angular value of the inter-revolution interval. For orbits with an easterly displacement of the flight trajectories the disruption of ordered observation is expressed in a progressive spreading apart of the scanning zones, which at a stipulated latitude φ does not make it possible to obtain an integral picture when investigating features whose dimensions exceed the l value. For solar-synchronous orbits a decrease in a_0 leads, in addition, to a disruption of the heliosynchronicity of precession of the orbital plane.

Thus, the admissible deviations of the semimajor axis from the nominal value are determined by the range of the acceptable Δl^* values, for example, $0.03 \leqslant \Delta l^*/l \leqslant 0.08$. With emergence of Δl^* beyond the limits of this range it is necessary to compensate for the accumulating secular perturbation of the semimajor axis.

The compensation methods can be different. The simplest is carrying out a single-impulse orbital correction with respect to the period of revolution with a simultaneous decrease in eccentricity. It is desirable that this method be used for space vehicles with a brief time of active operation during which it is necessary to carry out a limited number of such periodic corrections. For long-lived space vehicles a more rational method for maintaining the period of revolution, and especially with motion in solar-synchronous orbits, is a constant counteraction to the influence of the atmosphere by means of a low-thrust engine. This engine during the entire lifetime of the space vehicle must ensure a constant tangential acceleration whose value is equal to the perturbing acceleration caused by the effect of the atmosphere at the mean altitude of space vehicle flight.

We note that these obvious methods for maintaining the correctness of the scanning zones in the interrevolution interval can be used in combination with the possibilities of natural transfer between near-lying quasigeosynchronous trajectories with different order characteristics. It can be demonstrated, for example, that a space vehicle, situated initially in a circular orbit $N_3 = 44$ with an altitude 624 km and an inclination 81.4°, ensuring $\Delta L = 3.49°$, after three months of operation, as a result of a decrease of altitude in the atmosphere, passes without the application of correcting impulses to an orbit $N_4 = 59$, ensuring the same displacement of the flight trajectories. If the conditions for operation of the space vehicle require less time for implementation of transfer between orbits, it can be accelerated by means of impulse or low-thrust engines. After a double cycle of operation in both orbits the space vehicle can be returned to the initial orbit by use of these same engines.

Such a combined use of natural and forced interorbital transfers is possible for relatively long-lived space vehicles whose orbits are not solar-synchronous. Transfers can take place in periods of pauses caused by departures of the working branch of the trajectory from satisfactory illumination of the planetary surface.

In order to evaluate the transfer time and orbital parameters at the end of a maneuver it is possible to use formulas derived in [6]. Taking into account the small orbital ellipticity at the beginning of the active segment it is sufficient to use the following expressions for determining the end of this segment at the moment in time t, the semimajor axis $a_t = p_t/(1 - e_t^2)$, the eccentricity $e_t = \sqrt{h_t^2 + k_t^2}$, the argument of pericenter latitude $\omega_t = \operatorname{arctg}(h_t k_t)$, true anomaly $\vartheta_t = u - \omega_t$:

$$\left.\begin{aligned} p_t &= (C_p - 2\beta u)^{-1/2}, \\ h_t &= C_h p_t - \beta p_t^2 \cos u + \beta^2 p_t^4 \sin u + o(\beta^3 p_t^6), \\ k_t &= C_k p_t + \beta p_t^2 \sin u + \beta^2 p_t^4 \cos u + o(\beta^3 p_t^6), \end{aligned}\right\} \tag{8}$$

where

$$\left.\begin{aligned} C_p &= \frac{1}{p_a^2} + 2\beta u_a, \\ C_h &= \frac{1}{p_a}\left[h_a + \beta p_a^2 \cos u_a - \beta^2 p_a^4 \sin u_a + o(\beta^3 p_a^6)\right], \\ C_k &= \frac{1}{p_a}\left[k_a - \beta p_a^2 \sin u_a - \beta^2 p_a^4 \cos u_a + o(\beta^3 p_a^6)\right]. \end{aligned}\right\} \tag{9}$$

The duration of the maneuver is

$$t - t_a = \frac{2}{\beta\sqrt{fMp_a}}\left(1 - \sqrt{p_a/p_t}\right). \tag{10}$$

In formulas (8)-(10) $h_a = e_a \sin \omega_a$; $k_a = e_a \cos \omega_a$; $p_a = a_0(1 - e_a^2)$; $\beta = 2\tau/fM$, where τ is constant tangential acceleration developed by the low-thrust engine; u is the argument of space vehicle latitude, during maneuvering used as an independent variable; elements with the subscript a correspond to the beginning of the maneuver. The parameters a_a, e_a, ω_a, u_a, and also i_a and Ω_a are taken from a forecast of the passive motion of a space vehicle in the preceding flight stage in the time interval $\Delta t = t_a - t_0$, where t_0 is the time when the space vehicle is put into orbit. A forecast of motion in the model of the gravitational field which we adopted is possible, for example, using the formulas in [4], taking into account the nominal a_0 and i_0 values which we selected, taking into account the elements e_0, u_0 and ω_0 which are obtained as a result of putting a space vehicle into a working orbit in accordance with a known program, and finally, taking into account the longitude of the ascending node Ω_0, which is unambiguously determined by the time of carrier-rocket launching.

The applicability of expressions (8)-(10) in the considered problem is admissible due to the small thickness of the layer in which the active segment of the maneuver lies; this makes it possible to assume a constancy of the tangential braking acceleration from the effect of the atmosphere during the course of the entire interorbital transfer. The maneuver is continued to such a value of the variable u which leads to the attainment of an a_t value satisfying the condition (2), taking into account the corresponding requirements on displacement of the trajectories ΔL_t into a new quasigeosynchronous orbit.

It should be noted that $i_t = i_a$, $\Omega_t = \Omega_a + \Delta\Omega_t + \delta\Omega_t$, where $\Delta\Omega_t$ and $\delta\Omega_t$ is the secular and long-period change in the longitude of the ascending node during the time of maneuvering. An allowance for $\delta\Omega_t$ for increasing the accuracy in determining longitude Ω_t at the end of the active segment is desirable due to the fact that the transfer is accomplished in the neighborhood of resonance $1:N_m$. One of the methods for evaluation in the case of motion in the field of the fundamental zonal and individual tesseral harmonics of terrestrial gravity potential was proposed in [7].

It can be demonstrated that expressions (8)-(10) with the accuracy in computations of $o(\varepsilon^3)$ which we adopted are correct for any intermediate orbits, including for those which are obtained in model fields in [4, 7].

Thus, we have considered the peculiarities of trajectories of space vehicles intended for investigating the earth from space; methods for computing the nominal parameters of these trajectories; different methods, including interorbital maneuvering, reducing the orbital semimajor axis, decreasing under the influence of the atmosphere; methods for computing the active segments of interorbital transfers using low-thrust engines. All the formulas presented were derived with an accuracy to terms of the order of the square of the earth's flattening, which completely satisfies all the accuracy requirements in the stage of ballistic planning of the considered space vehicles. All the formulas cited here and recommended for use are easily programmed and do not require great expenditures of computer time.

BIBLIOGRAPHY

1. Takahashi, Kozo, "Determination of Elements of Sub-synchronous or Super-synchronous Orbits and Their Application to Operational Satellites," J. RADIO RES. LAB., Vol 22, No 108, pp 45-57, 1975.

2. Grishin, S. D., Zhuravlev, I. F., Lisovoy, V. T., Saul'skiy, V. K., Surikov, V. M., "Choice of Artificial Earth Satellite Orbits for Investigating the Earth's Natural Resources," KOSMICHESKIYE ISSLEDOVANIYA ZEMNYKH RESURSOV (Space Investigations of the Earth's Resources), Moscow, "Nauka," pp 310-316, 1975.

3. Lukashevich, Ye. L., "Planning of Orbits of Geodetic Space Vehicles," GEODEZIYA I KARTOGRAFIYA (Geodesy and Cartography), No 7, pp 18-22, 1979.

4. Lukashevich, Ye. L., "One Integrable Case of Satellite Motion in the Acentral Terrestrial Gravitational Field," KOSMICH. ISSLED. (Space Research), Vol 17, No 3, pp 457-459, 1979.

5. El'yasberg, P. Ye., VVEDENIYE V TEORIYU POLETA ISKUSSTVENNYKH SPUTNIKOV ZEMLI (Introduction to the Theory of the Flight of Artificial Earth Satellites), Moscow, "Nauka," 1965.

6. Lukashevich, Ye. L., "Analysis of Motion in a Central Field Under the Influence of Small Acceleration," TRUDY 8-kh CHTENIY, POSVYASHCH. RAZRAB. NAUCH. NASLEDIYA I RAZVITIYU IDEY K. E. TSIOLKOVSKOGO, KALUGA, 1973 SEKTS. MEKH. KOSMICH. POLETA (Transactions of the Eighth Readings Devoted to the Development of the Scientific Heritage and Development of the Ideas of K. E. Tsiolkovskiy, Kaluga, 1973 Section on the Mechanics of Space Flight), Moscow, pp 130-140, 1974.

7. Lukashevich, Ye. L., "Integrable Case of Motion of an Artificial Earth Satellite With Allowance for the Influence of Longitudinal Terms in Gravitational Potential," KOSMICH. ISSLED. (Space Research), Vol XVII, No 6, pp 929-931, 1979.

[352-5303]

5303
CSO: 1866

UDC 551.501:629.195.1

METEOROLOGICAL SOUNDING OF THE SUBJACENT SURFACE FROM SPACE

Leningrad METEOROLOGICHESKOYE ZONDIROVANIYE PODSTILAYUSHCHEY POVERKHNOSTI IZ KOSMOSA (Meteorological Sounding of the Subjacent Surface from Space) in Russian 1979 signed to press 1 Nov 79 pp 2, 247

[Annotation and Table of Contents from the book by K. Ya. Kondrat'yev, Al. A. Grigor'yev, Yu. I. Rabinovich and Ye. M. Shul'gina, Gidrometeoizdat, 1,150 copies, 247 pages]

[Text] The state of the art in remote sensing of the characteristics of an underlying surface from space (dry land and oceans), which are of the greatest importance from the viewpoint of accounting for the interaction of the atmosphere and the subjacent surface in the study of weather and climate is discussed. The possibilities for the interpretation of images in various regions of the spectrum for the purpose of studying water basins, snow and ice cover as well as vegetation are examined. The methods and results of reproducing the temperature of the underlying surface from the measurement data of the emitted radiation in the transmittance windows of the atmosphere are analyzed in detail. A considerable portion of the monograph is devoted to questions of the remote determination of the parameters of the underlying surface and the upper layer of the soil based on data of radiothermal emission measurements.

The monograph is of interest to students in advanced courses and graduate students specializing in the field of meterology, climatology and space research as well as specialists in related fields.

Table of Contents

[337-8225]

8225
CSO: 1866

MATERIALS PROCESSING IN SPACE

Moscow MATERIALY I PROTSESSY KOSMICHESKOY TEKHNOLOGII (Materials and Space Technology Processes) in Russian 1980 signed to press 21 Nov 79 pp 3-4, 221-222

[Foreward and table of contents from book edited by A. S. Okhotin, Izdatel'stvo "Nauka", 229 pages]

[Text] The analysis of materials formed in zero gravity has been reduced, in essence, to analyzing previously performed experiments and, in some cases, to attempts to explain the observed anomalies. This work is by no means complete and, evidently, the next step in the analysis will be the transition from particular interpretations to a generalized examination of all aspects of the problem. One of the basic factors here will be the construction of qualitative and quantitative theoretical models that explain the experimental results. This work has only just begun and, from the point of view of the experiments that have already been performed, theory can only describe the results obtained, since the anomalies that often arise in the materials of space technology are caused not by the peculiarities of a process per se, but by imperfections in the equipment. It is now important to "put everything in its place" (and this is already being done), i.e., theoretical studies must lead and determine the setup of an experiment. For this reason, theoretical studies in the area of space technology are now mainly directed toward analyzing the flow of transport processes in liquids and gases, as well as the processes of crystallization and condensation of substances in zero gravity for the most diverse structures.

The problems in preparing new experiments naturally involve a wider range of problems (ground-based studies of the most diverse materials that it would be expedient to produce in space; development of methods for modeling the properties of materials for space technology, as well as methods for studying these materials; development of equipment for processing in zero gravity). These problems are directly related to such problems as creating energy sources that are more powerful than those currently used on space stations, the behavior of various materials in space, and so on.

All the problems cited above are, to one degree or another, reflected in this collection of articles, which directs a great deal of attention toward a consideration of the processes for fabricating materials in space and studying their physicochemical properties. The experimental results concerning shaping during metallic fusion at the time of the Soyuz-Apollo" flight, as well as the results of work on particular aspects of fabricating optical glass in zero gravity, are generalized. The causes of high porosity in metals smelted in space are studied. The peculiarities of crystal growth from vapor-gas media in zero gravity are examined. The effect of a gradient in the surface tension on the processes occurring in the meniscus while growing crystals from a melt, as well as the effect of the shape of the crystallization front on the concentration profile in a solid, and other similar problems are considered. Among the articles concerning material properties, a series of articles dealing with methods for studying the thermophysical characteristics of semiconducting film and bulk specimens are of interest. It is important that the techniques developed for studying the materials of space technology can be used for making measurements on a broad class of semiconductors and metals. The main articles dealing with the behavior of materials in space are concerned with the study of the effect of radiation on semiconductors and polymers. These works can be useful in creating models that simulate conditions in space, as well as for creating models of the mechanism for the action of radiation on solids.

In articles concerned with possible methods for providing energy for processes in space technology, several aspects of the prolonged operation of nuclear and isotopic thermogenerators are examined.

As a whole, this collection is a logical extension of two previous collections, Materials Processing and Technology in Space and The Fabrication and Behavior of Materials in Space, published by "Nauka" in 1977-1978.

The Editors

Contents

Page

Page

[145-9638]

9638
CSO: 1842

UDC 631.4

AEROSPACE METHODS OF STUDYING SOILS

Moscow AEROKOSMICHESKIYE METODY IZUCHENIYA POCHV (Aerospace Methods of Studying Soils) in Russian 1979 signed to press 14 Dec 79 pp 2, 4-6, 279-280

[Annotation, introduction and table of contents from the book by V. L. Andronikov, [Izdatel'stvo "Kolos"], 3,400 copies, 280 pages

[Text] The theoretical principles of methods of deciphering the soil cover based on its imagery in photographs from aerospace photography of the earth's surface are treated in this book. Questions of the utilization of multizonal and multispectral photographic materials for soil study are presented for the first time.

Introduction

The use of aerospace materials for the study of soil cover is attracting the attention of Soviet and foreign researchers at the present time.

The necessity of broadening research on the applications of space tools to the study of the natural resources of the earth was indicated in the "Basic Developmental Trends for the USSR National Economy During 1976-1980". Remote aerospace methods are objective high speed automated systems for data gathering and processing concerning the condition of soils and agricultural lands and plantings.

The management of agricultural production can be organized more efficiently on this basis.

One of the new trends in the field of the application of aerospace methods to soil and agricultural crop studies is the development of multizonal and multispectral aerospace photography. It consists in the photography of the same section of ground surface simultaneously in several narrow bands of the spectral. As a result, photographs are obtained which contain the maximum information on the soil cover and agricultural crops.

The agricultural applications (for the study of soil cover and plantings) of infrared photographic, photoelectronic and radar images are promising.

The latter can function in the absence of visibility (through clouds and even at night). The humidity, certain structural elements and the composition of soil cover, as well as the make-up of the upper levels and the kinds of agricultural crops are determined from radar images.

Space photography of the soil cover and agricultural crops, as compared to aerial photography, makes it possible for the first time to objectively see the soils and the agricultural crops simultaneously over large territories, individual mountain ranges and the vertical layered structure of soil and vegetative cover, as well as the nature of irrigation and drainage systems as a whole. Another important specific feature of space photography lies in the fact that there is an objective generalization of the soil cover in space photographs, and moreover, these photographs make it possible to interpret the soil cover in individual, frequently remote regions. The utilization of space materials will assist in a more in-depth and objective study of soils.

One of the major fundamental features of photography from space is the operational timeliness in obtaining information on the status of soil cover, the nature of snow thawing, the development of erosion processes and the status of agricultural crops on a national scale. Yet another specific feature of space photography lies in the possibility of rapidly repeating the photography. This is especially important for assessing rapidly developing dynamic soil and agricultural processes occurring on the earth's surface.

Aerospace (remote) methods using the appropriate receivers installed in an aircraft and space vehicle, on one hand, record the reflection of sunlight from soils and vegetation, and on the other hand, pick up the inherent radiation of the soil and vegetative cover of the earth's surface.

The utilization of aerospace methods is based on the fact that the absorption, radiation, scattering and reflection of electromagnetic energy by various soils and plantings is selective and specific for each soil and agricultural crop.

The interpretation of the soil cover is accomplished from its images on aerial and space photographs, including multizonal ones. In this case, the interpretability and possibilities for the use of aerospace photographs obtained in different bands of the electromagnetic spectrum for the study of the soil cover are also studied and determinants are developed for the interpretation of soils.

Studies on soil interpretation were conducted on the territories of the steppe, dry steppe and desert regions of our nation.

Studies of the interpretation of soil cover, agricultural crops and virgin vegetation were made using black and white, color and spectral band aerial photographs, multiband aerial photographs (green, red and infrared bands), obtained using the AFA-39M set during photographing in 1973-1975, multispectrum aerial photographs obtained with a scanner and black and white space photographs from the "Soyuz-9", "Salyut-1" and "Salyut-4", multiband space photographs from the "Soyuz-12", "Salyut-4", "Soyuz-22" as well as from the experimental "Meteor" satellites.

Also analyzed in the work were the foreign black and white and color space photographs from the "Gemini" and "Apollo" satellites, as well as multispectral space photographs in four bands of the spectrum from the ERTS satellite, the "Landsat", taken for the territories of the USSR and foreign countries.

The combined utilization of aerial and space photographs is the optimal variant for the interpretation of soil cover and vegetation images. In this case, the interpretation of the aerial photographs is most successfully utilized in key areas to study the structural components of soil cover, while in the interpretation of space photographs, soil scientists come up against a generalized image of the soil surface. The study and interpretation of aerial and space photographs begin with a preliminary laboratory period, the significance of which increases with the use of multiband photographs, as well as stereoscopic, optronic and photometric equipment for processing photographs and films.

The interpretation of aerospace photographs included field work on the ground to study the soil cover and plantings of agricultural crops, as well as to check the results of laboratory interpretation. Materials from a book on the history of the fields, taking into acccount crop yield data, were used in the work. The existing soil and topographical maps with different scales, plans showing the placement of agricultural crops and materials from the literature were used in the laboratory and field interpretation, in addition to the field research data.

The steroscopic method was used to analyze the aerospace materials, employing a stereoscope and a photointerpretation unit. The spectral reflectivity of soils was measured for air dried samples using the SF-10 spectrophotometer. The MF-4 microphotometer was used in studying the aerospace photographs, and a quantitative visual and instrumental interpretation procedure was employed using the modern "Kvantimet-720" electronic-optical image meter and analyzer. The chemical analyses of the soils were performed in the mass analysis laboratory of the Soil Institute. Besides the experimental photographs made by the Soil Institute, the materials of the multizonal experimental flights of the Institute of Space Research of the USSR Academy of Sciences were also widely used in the work. A considerable portion of the space photographs were made available by the "Priroda" State Center of the GUGK of the Main Administration for Geodesy and Cartography of the USSR Council of

Ministers and the GosNITsIPR of the USSR State Committee on hydrometeorology and monitoring of the natural environment.

Table of Contents

8225
CSO: 1866

UDC 684.932:528.7.004.13

THE STUDY OF TAIGA TOPOGRAPHY BY REMOTE METHODS

Novosibirsk ISSLEDOVANIYE TAYEZHNYKH LANDSHAFTOV DISTANTSIONNYMI METODAMI (Studying Taiga Topography by Remote Methods) in Russian 1979 signed to press 4 Jul 79 pp 2, 214

[Annotation and Table of Contents from the book edited by A. S. Isayev, Izdatel'stvo Nauka, Siberian Department, 1,000 copies, 216 pages]

[Text] The results of studies of the taiga topography of Siberia using aerospace methods are given in this collection. Questions of the theory of structural topographical interpretation of photographs and dynamic phenomena are treated (the dynamics of the interrelationships of forest and bog, the age and pyrogenic dynamics of forests, hydrological dynamics and the phenological status of plants). Considerable attention is devoted to methodological questions of mapping natural and territorial complexes, forests, soils, bogs and past fires. Methods of mathematically processing data obtained during the interpretation of photographs in forest survey and biometric studies are examined.

The collection is intended for scientists and specialists in various professions: geographers, topographers, foresters, soil scientists, swamp specialists and geobotanists.

Table of Contents

8225
CSO: 1866

SPACE ENGINEERING

SYSTEM FOR THE EMERGENCY RESCUE OF COSMONAUTS FROM ORBITAL STATIONS [SASKOS]

Moscow TRUDY ODINNADTSATYKH CHTENIY, POSVYASHCHENNYKH RAZRABOTKE NAUCHNOGO NASLEDIYA I RAZVITIYU IDEY K.E. TSIOLKOVSKOGO (KALUGA, 14-17 SEP1976), SEKTSIYA "PROBLEMY RAKETNOY I KOSMICHESKOY TEKHNIKI" in Russian, 1978 pp 101-108

[Paper by Belonogov, Ye.K., Ivarovskiy, S.A., Grigorovich, V.K., Zatsepin, A.Yu., Ignat'yev, V.V., Sokolov, V.A., Tarasov, V.N., and Minenko, V.Ye., USSR Academy of Sciences, Commission for the Development of the Scientific Heritage of K.E. Tsiolkovskiy]

[Text] The successful work of crews on board orbital space stations (OS) and the valuable results of the scientific research confirm the foresight of K.E. Tsiolkovskiy concerning the necessity of organizing large orbital stations, which he called "space settlements" [1, p 301]. In his works "The Exploration of Outer Space by Means of Reaction Motors", "The Goals of Star Travel" and "Beyond the Earth", Tsiolkovskiy not only provided a theoretical basis for the possibility of space station design, but also cited various orbital station configurations, described ways of changing crews and treated numerous other questions.

Tsiolkovskiy repeatedly underscored the fact that for the mastery of outer space "special accomodations are needed - safe ones, . . . with conveniences for life and work" [1, p 302]. In our time, the group of problems, for the solution of which a major role is assigned to space vehicles, is expanding rapidly. The crews of orbital stations survey the natural resources of the earth, gather information needed for agriculture, forest management, geology and meteorology, as well as study the sun and the planets of the solar system.

Considerable attention is being devoted to flight safety in the design of all manned space systems [2]. In the future, when the duration of orbital station missions will increase, and the increased activity of

mankind in space will lead to multiple "earth to space station orbit" shuttle flight operations, it will not be expedient to execute the orbital mission with the shuttle craft docked with the station.

Along with this, because of the increased complexity of station systems and structures, the probability of the occurrence of emergency situations on board a space station is increased. In a number of cases, the docking of an orbital station to a shuttle rescue ship can prove to be impossible. For this reason, it is expedient to have independent means of safely returning the station crew by means of special space vehicles (capsules) along with the regular transport ships.

The results of planning and structural design work on a possible variant for a rescue capsule, located on board an orbital station, are given in this paper. The major function of the emergency rescue capsule consists in providing for the evacuation of the crew of the orbital space station in the case damage occurs which cannot be eliminated.

The project design for the Saskos was carried out for the following initial data:

--The initial altitude of the circular orbit	400 km
--The number of capsule crew members	3 persons
--Autonomy of the life support system	24 hours

--Descent in the atmosphere -- uncontrolled, ballistic (lift-to-drag ratio = 0), maximum G force ≈ 9

--The landing is on dry land or a water surface.

Calculations of the following were made in the design of the capsule: the aerodynamic characteristics of the capsule [3], the portions of the trajectory outside and inside the atmosphere [4, 5], the solid fuel braking engine [6], the parachute system [7] and the size and weight characteristics of the life support system [8]. The results of the ballistic design calculations are shown in Figure 1. As can be seen from the results presented here, the maximum thermal flux (at the critical point) amounts to about 555 KW/m^2. In this case, the maximum equilibrium temperature does not exceed 1,770° K.

The parameters for the heating of the structure which were found make it possible to use a panel made of honeycomb glass matrices for the heat shielding of the capsule, the cells of which are filled with a light foam material based on rubber type silicone polymers which include in

their composition galss fibers or other fillers which improve the thermal insulation characteristics of the material.

The planning and design work which has been done has made it possible to determine the major weight (Table 1) and structural design (Table 2) characteristics, as well as the configuration of the systems installed in the capsule, in particular, the landing, life support, control, engine systems, etc.

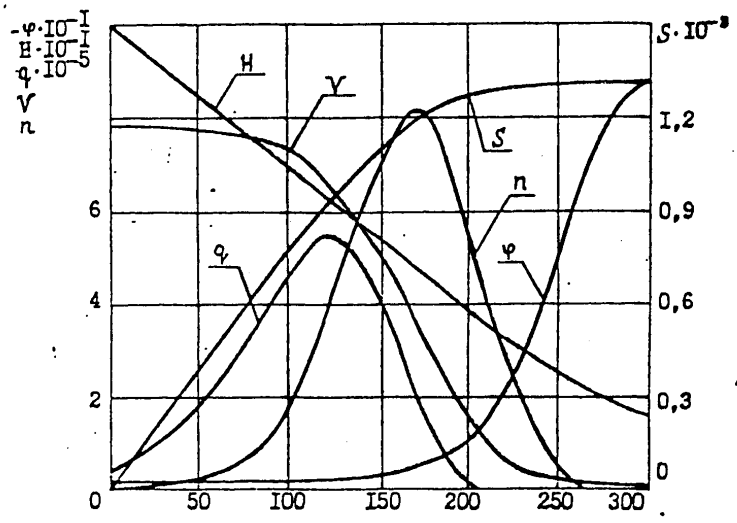

Figure 1. The results of the ballistic design calculations:

H is the altitude [km];
v is the capsule velocity [km/sec];
q is the specific heat flux [w/m^2];
S is the range of the atmospheric flight phase [km];
n is the G-loading.

TABLE 1 The Weight Characteristics of the Capsule

1. The total weight of the capsule	1,260 kg
2. The crew (in spacesuits)	270 kg
3. The control and orientation system	95 kg
4. The life support system	95 kg
5. The braking engine	115 kg
6. The landing system	100 kg

7. The power equipment	35 kg
8. Structural components	130 kg
9. Heat shielding	420 kg

TABLE 2 The Major Structural Design Characteristics of the Capsule

1. Requisite braking impulse	143 m/sec
2. Atmospheric entry angle (H = 100 km)	-2°
3. Load on the support surface	90 kg/m^2
4. Drag coefficient	1.70
5. Maximum specific heat flux	555 KW/m^2
6. Vertical velocity of parachute supported fall at the earth	7 m/sec
7. The calculated landing (or water landing) velocity	0 to 3 m/sec
8. Structural material AMg6	

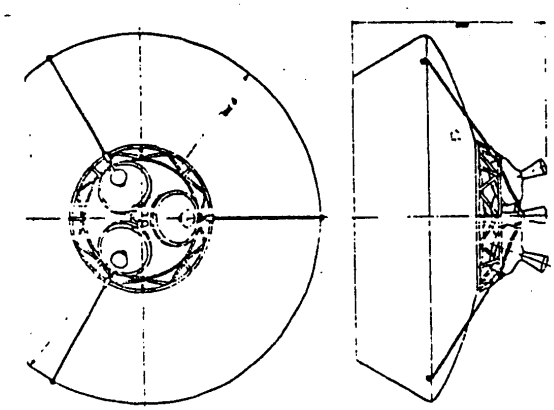

Figure 2.

The cosmonaut emergency rescue system structurally consists of a container on the orbital station and a capsule, which is docked with the container. An overall view of the capsule is shown in Figure 2. The major structural component of the Saskos capsule is the heat shield, which is made in the form of a spherical segment. The motion of the vehicle is stable throughout the entire range of descent velocities, while its dimensions provide for comparatively light loading on the

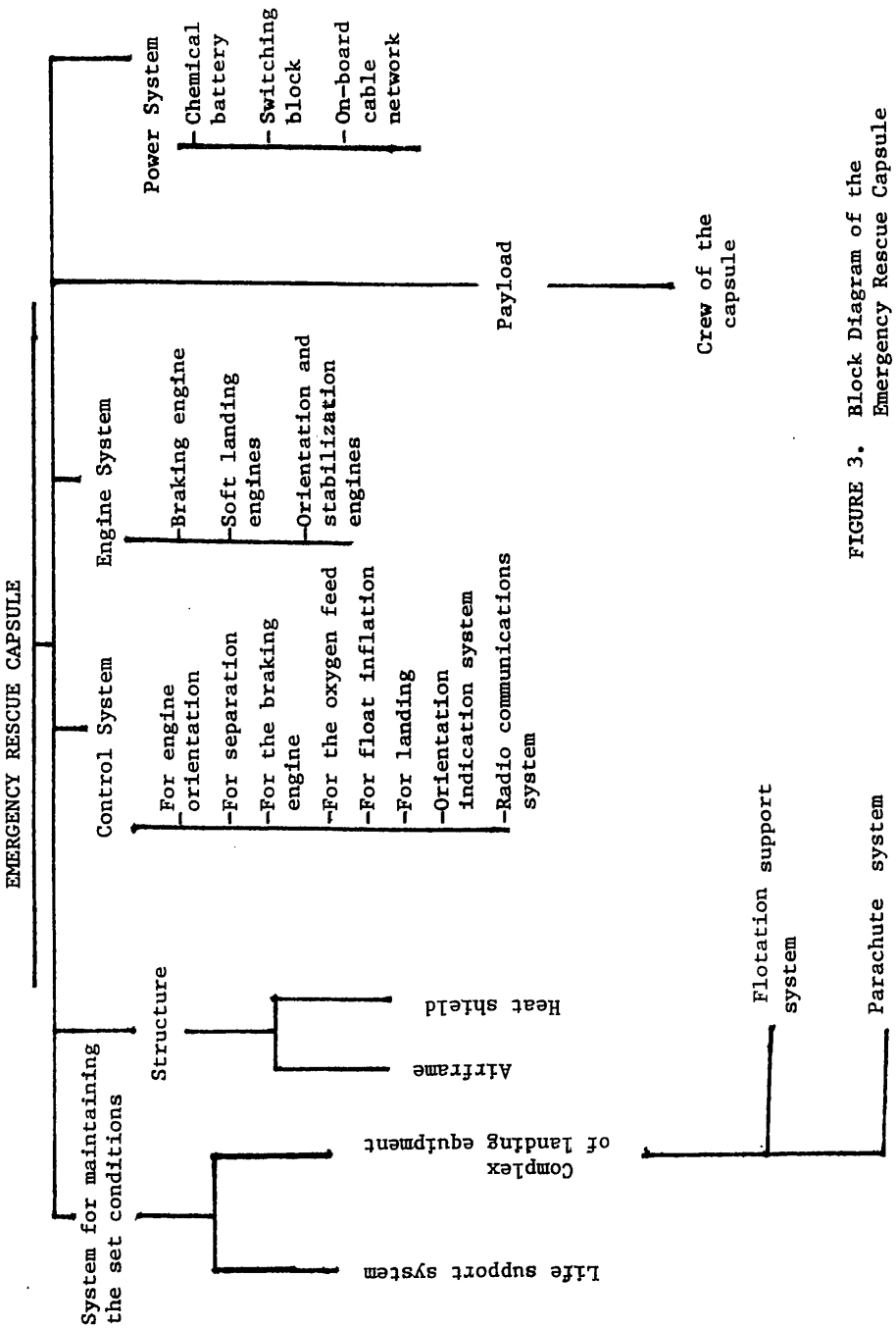

FIGURE 3. Block Diagram of the Emergency Rescue Capsule

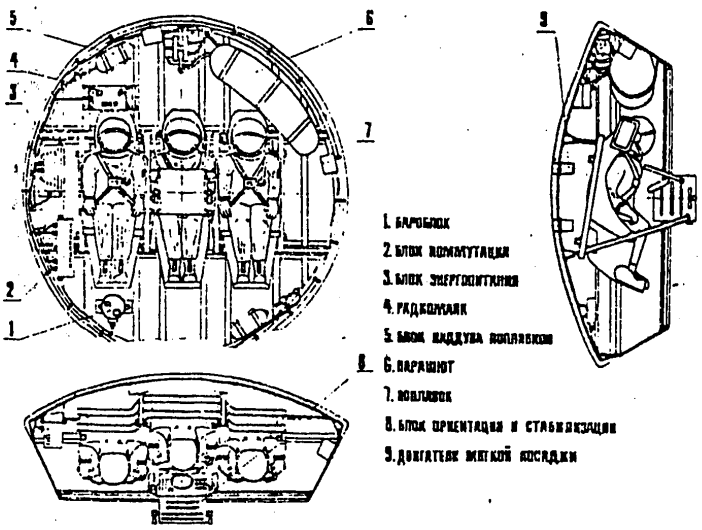

Figure 4.

Key: 1. Barometric unit;
2. Switching unit;
3. Power supply;
4. Radio beacon;
5. Flotation inflation unit;
6. Parachute;
7. Float;
8. Orientation and stabilization unit;
9. Soft landing engines.

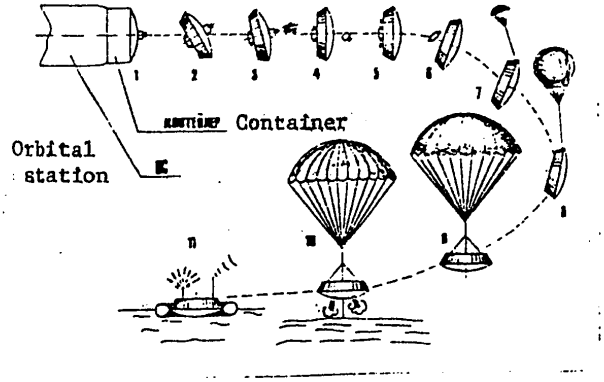

Figure 5.

support surface. The cosmonauts are placed in the convex surface of the heat shield in special couches, as well as the systems which provide for the descent and life support maintenance of the crew. A block diagram of the Saskos capsule is shown in Figure 3, the layout is shown in Figure 4, while a functional depiction is shown in Figure 5.

In the case of an emergency situaiton in an orbital station, the crew in spacesuits enters the capsule. The capsule separates from the station by means of spring pushers and moves away from it. Then the pilot, sitting in the center seat, sets the orientation and stabilization unit in the working position and orients the capsule (position 2) using the visual orientation sight, after which the automatic unit is engaged which fires the main engine (DU) (position 3). After the requisite braking impulse for descent from orbit is obtained, the engine is jettisoned (Figure 4). Prior to entering the dense layers of the atmosphere, the orienting of the capsule is repeated (position 5). The orientation and stabilization unit for the capsule is used both in the initial flight trajectory and in the dense layers of the atmosphere; it is then fired clear by means of explosive pushers (position 6). After going through the aerodynamic braking portion of the trajectory, which is characterized by peaks in the G-loading and the heat flux, the parachute system is actuated at an altitude of 9 to 11 km. A stablizing canopy is deployed on an instruction from the barometric unit (position 7), which pulls out the main parachute, which is reefed and functions as a braking parachute (position 8). When a velocity of 25 to 30 m/sec is reached, the reefing is pulled out and smooth parachuting at a velocity of about 7 m/sec to the surface of the earth begins (position 9). During the free parachuting time, signals are transmitted by means of the antenna in the parachute shroud line for DFing the capsule. At the same time as the opening of the main canopy, an explosive cartridge fires which ejects the pin-transducer for turning on the soft landing engines.

When the transducer touches the ground or a water surface, the instruction is given for firing the soft landing engines which cancel the vertical component of the capsule velocity (position 10). The float containers are simultaneously inflated which provide for vehicle flotation. Following the landing (or water landing), an explosive lock actuates which jettisones the direction finding radio beacon antenna, and the flashlamp for the light signaling system is deployed for purposes of facilitating the detection of the vehicle (position 11). In the case of landing in an unplanned region, there is an emergency supply of water and food, a first aid kit, etc. on board the capsule.

To be included among the merits of this SASKOS variant are complete independence of the capsule, control simplicity, as well as comparatively low cost in the realization of the given design.

BIBLIOGRAPHY

1. "The Exploration of Outer Space by means of Reaction Motors" (Republication of the 1903 and 1911 works with some addenda and emendations), in the collection, "Izbrannyye trudy" ["Collected Works"], Moscow, 1962, pp 242-327.

2. R.A. Stasevich, "Evaluating Space Flight Safety", in the book, "Idei Tsiolkovskogo i problemy kosmonavtiki. Izbrannyye trudy I-V Chteniy K.E. Tsiolkovskogo" ["The Ideas of Tsiolkovskiy and Problems of Astronautics. Selected Works of Readings I - V of K.E. Tsiolkovskiy", Moscow, 1974, pp 129-135.

3. N.F. Krasnov, "Aerodinamika raket" ["The Aerodynamics of Rockets"], Moscow, 1968.

4. P.Ye. El'yasberg, "Vvedeniye v teoriyu poleta iskusstvennykh sputnikov zemli" ["Introduction to the Theory of Flight of Artificial Earth Satellites"], Moscow, 1965.

5. I.I. Drakin, "Aerodinamicheskiy i luchistyy nagrev v polete" ["Aerodynamic and Radiative Heating in Flight"], Moscow, 1961.

6. A.M. Vinitskiy, "Raketnyye dvigateli na tverdom toplive" ["Solid Fuel Rocket Engines"], Moscow, 1973.

7. S.M. Alekseyev, et al., "Sovremennye sredstva avariynogo pokidaniya samoleta" ["Modern Means of Abandoning an Aircraft in an Emergency"], Moscow, 1961.

8. S.M. Alekseyev, S.P. Umanskiy, "Vysotnyye i kosmicheskiye skafandry" ["High Altitude and Space Suits"], Moscow, 1973.

[8144/1466-8225]

8225
CSO: 8144/1466

UDC 522.59

ON APERTURE SYNTHESIS USING A SPACE RADIOTELESCOPE

Moscow ASTRONOMICHESKIY ZHURNAL in Russian Vol 57, No 3, 1980 manuscript received 15 May 79 pp 634-648

/Article by N.S. Kardashev, S.V. Pogrebenko and G.S. Tsarevskiy, Institute of Space Research, USSR Academy of Sciences/

/Text/ It is possible to obtain unambiguous radio images of sources that are independent of modeling concepts with the help of aperture synthesis systems with good coverage of the spatial frequency spectrum. In this article the authors discuss an interferometer consisting of one ground-based and one low-orbital space radiotelescope (the RAKSAS-1 system). They describe the algorithm for the numerical modeling of the process of spatial frequency spectrum (uv-plane) coverage, present the results of the calculations, and analyze them. They also compare the information characteristics of the RAKSAS-1 with those of radiointerferometers of the RSDB and GRT (global radiotelescope) types. It is shown that the two-element RAKSAS-1 system has some advantages over multielement ground-based aperture synthesis systems as far as the degree of uv-plane coverage is concerned. The conditions for optimizing the process of obtaining radio images of sources are determined. Space interferometers offer the prospect of a practically unlimited increase in spatial resolution.

1. Formulation of the Problem

In recent years, more and more attention has been given to the development of promising radioastronomy systems for use in space /1-4/. Space radioastronomy systems offer practically unlimited possibilities for enlarging the collecting areas of antennas, in combination with the possibility of synthesizing high-quality two- and even three-dimensional /5,6/ radio images with a degree of resolution that cannot be achieved under terrestrial conditions. In connection with this, it is of interest to discuss some of the information possibilities of a space radioastronomy aperture synthesis

system (RAKSAS, for short) consisting of ground-based (NRT) and space (KRT) radiotelescopes.

Here we will discuss a possible initial version of this space radioastronomy system (which we will call RAKSAS-1) that includes a KRT circling the Earth in a low orbit (H = 300-400 km). Because of the high relative rate of motion of the terrestrial and space antennas of this radiointerferometer, the spatial frequency spectrum will be covered comparatively rapidly. In connection with this, the antennas participate in a complex relative motion that is -- generally speaking -- nonperiodic, which makes it possible to obtain a quite complete spatial frequency spectrum. This, in turn, has a substantial effect on the nonambiguity and quality of the images that are obtained /7,8/. A similar problem is encountered during the processing and interpretation of data obtained with ground-based interferometers that are used to synthesize the Earth's rotation. For the latter, an elliptical shape of the tracks of the base vector's motion in the plane of spatial frequencies (the uv-plane), with a period of 12 hours, is typical /9/. Since the track repeats in each subsequent period, the degree of uv-plane coverage by a ground-based interferometer consisting of a small number of antennas in ver low (see below). In contrast to this, with RAKSAS-1 there is practically complete and unicompendent coverage of a corresponding area of the uv-plane, the boundary of which is close to that of an ellipse.

In order to investigate the process of spatial frequency spectrum coverage in RAKSAS-1 and to compare it with the coverage provided by ground-based aperture synthesis systems consisting of two (type VLBI) and many (type VLBA) antennas, a series of numerical modeling programs was formulated. Below we present a brief description of the algorithms (Section 2) and the results of the modeling and a discussion of them (Section 3). A description and listing of the programs is presented in /10/.

2. Description of the Modeling Algorithm

2.1. Coordinate System and Equations of Motion. The motion of the aperture synthesis system's elements is discussed in the following rectangular coordinate system OXYZ, which is used to describe both radiointerferometers and the motion of AES /artificial Earth satellite/: the center of the coordinate system is placed at the center of the Earth, the OZ axis is directed toward the North Pole, the OX axis toward the point of the vernal equinox, and the OY axis completes the system of coordinates on the left.

In this system of coordinates, the equations of motion of ground-based radiotelescopes have the form

$$R_n^{(i)}(t)=\begin{cases} x_n^{(i)}(t)=R_e\cos\varphi_i\cos(\Omega t+\lambda_i+\lambda_0), \\ y_n^{(i)}(t)=R_e\cos\varphi_i\sin(\Omega t+\lambda_i+\lambda_0), \\ z_n^{(i)}(t)=R_e\sin\varphi_i, \end{cases} \quad (1)$$

where R_e = radius of the Earth; Ω = angular speed of rotation of the Earth; φ_i, λ_i = geographical latitude and longitude of the i-th NRT; λ_0 = angle between the point of the vernal equinox and the prime meridian at the origin of time.

Assuming a circular orbit and the absence of orbital precession and nutation, the KRT's equations of motion have the form /11/

$$\mathbf{R}_k(t)=\begin{cases} x_k(t)=R_0[\cos(\omega t+\vartheta_0)\cos\Omega_0-\cos i\sin(\omega t+\vartheta_0)\sin\Omega_0], \\ y_k(t)=R_0[\cos(\omega t+\vartheta_0)\sin\Omega_0+\cos i\sin(\omega t+\vartheta_0)\cos\Omega_0], \\ z_k(t)=R_0\sin i\sin(\omega t+\vartheta_0), \end{cases} \tag{2}$$

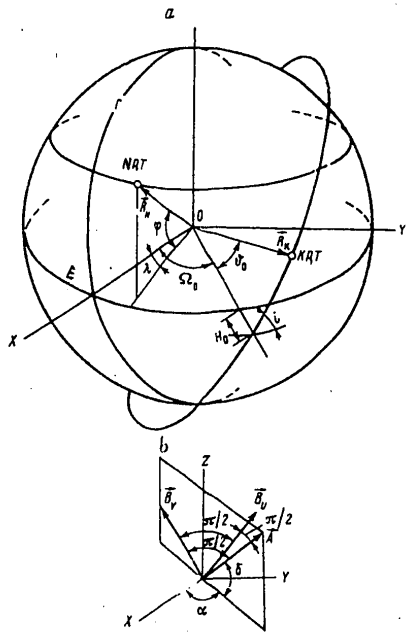

Figure 1. Geometry of space radioastronomy aperture synthesis system (RAKSAS-1): a. mutual position of ground-based and space-borne radiotelescopes (E = Earth's equator; G = Greenwich meridian); b. diagram for selection of basis in the uv-plane. For other definitions, see text.

where R_0 = radius of the KRT's orbit; ω = angular rate of motion of the KRT along its orbit; ϑ_0 = initial phase of motion of the KRT; Ω_0 = longitude of the orbit's ascending node; i = angle of inclination of the orbital plane to the Earth's equatorial plane.

The effect of precession of the KRT's orbital plane on the result of uv-plane coverage can be allowed for by introducing a dependence of Ω_0 on time, although (as will be seen below) for observations with duration $T_0 \sim 1$ day, it is possible not to allow for precession.

The equations of motion for the NRT-KRT and NRT(i)-NRT(j) bases have the form

$$\mathbf{B}_{nk}(t)=\mathbf{R}_k(t)-\mathbf{R}_n(t),$$
$$\mathbf{B}_{nn}^{(ij)}(t)=\mathbf{R}_n^{(i)}(t)-\mathbf{R}_n^{(j)}(t) \tag{3}$$

(subscript "n" means ground-based, "k" means space-borne).

The approximate geometry of the mutual position and motion of the RAKSAS-1 system is shown in Figure 1a.

2.2. The Observed Object and the Basis in the uv-Plane. The location of the observed object in the celestial sphere is given in coordinates α (right ascension) and δ (declination). The direction vector A to the object is defined as

$$\mathbf{A}=\begin{cases} A_x=\cos\alpha\cos\delta, \\ A_y=\sin\alpha\cos\delta, \\ A_z=\sin\delta. \end{cases} \tag{4}$$

The plane of observation (a spatial analog of the uv-plane) is given as the plane that passes through the origin of the coordinate system and is perpendicular to vector A. The basis vectors in the plane of observation (or in the uv-plane, which is the same with a degree of accuracy up to that of the dimensionality) are chosen as

$$\mathbf{B}_v=\begin{cases} B_{vx}=\cos\alpha\cos(\delta+\pi/2), \\ B_{vy}=\sin\alpha\cos(\delta+\pi/2), \\ B_{vz}=\sin(\delta+\pi/2), \\ \mathbf{B}_u=[\mathbf{B}_v\times\mathbf{A}], \end{cases} \tag{5}$$

that is, vector B is formed from A by rotating it 90° in the plane passing through A and the OZ axis. Vectors A, B_u and B_V form an orthonormal basis, in connection with which the projection of the system's base's vector on B_V determines the resolution with respect to coordinate α, while the projection on B_V does the same with respect to coordinate δ and the projection on A determines the difference in the signal's path (lag) from the source to one of the radiotelescopes relative to the other. The diagram for selecting the basis in the uv-plane is shown in Figure 1b.

2.3. Allowing for Simultaneous Visibility of the Object. For an NRT, the condition of source "visibility" means that the radiotelescope is on the same side -- relative to the plane of observation -- as the observed object, and for this it is necessary that the following condition be fulfilled:

$$(\mathbf{R}_n^{(i)}\cdot\mathbf{A})>0. \tag{6}$$

Depending on the altitude of its orbit, the KRT will "see" the source for some time after it moves to the opposite -- relative to the source -- side of the plane of observation, until it enters the cylinder of shade created by the Earth. Thus, the condition for the cessation of source visibility by the space radiotelescope can be written in the form

$$\{(\mathbf{R}_k\cdot\mathbf{A})\leqslant 0\}\cap\{(\mathbf{R}_k\cdot\mathbf{B}_u)^2+(\mathbf{R}_k\cdot\mathbf{B}_v)^2-\mathbf{R}_e^2\leqslant 0\}. \tag{7}$$

In the modeling process, coverage of the uv-plane by a pair of telescopes is interrupted if even one of them cannot "see" the object at the given moment.

2.4. Processing of the Modeling Results. For the processing of the modeling data, the following parameters are defined: number of cells covered = N; maximum base realizable in a given numerical experiment = B_{max}; time utilization factor (that is, the part of the time during which simultaneous visibility of the investigated object by both radiotelescopes is realized) = K_t.

In addition to this, the function $\Phi(t_c)$ of the distribution of the number of cells covered with respect to the accumulation time t_c for a single cell is also defined.

In the analysis of the different interferometric systems, it is convenient to use their information content as the comparison parameter. Information content S corresponding to the spatial frequency filter, which depends on the nature and degree of coverage of the uv-plane, has been defined by (Shennon) as

$$S=\sum_{ij}\ln[1+(F/\sigma_F)_{ij}]\Delta u\,\Delta v, \tag{8}$$

where $(F/\sigma_F)_{ij}$ = signal-to-noise ratio in the (i,j)-th cell of the discrete uv-plane; Δu, Δv = linear dimensions of a cell. For $F/\sigma_F \ll 1$ (a weak source), we can limit ourselves to the first term of the expansion of the logarithm into a Taylor series; considering the fact that $F/\sigma_F \sim t_c^{1/2}$, we obtain

$$S_1=\Delta u\,\Delta v\sum_{ij}t_c^{1/2}. \tag{9}$$

In the case of a strong source, $F/\sigma_F \gg 1$ and the logarithm in formula (8) can be ignored in comparison with the "information" term, which is linearly dependent on the number of cells covered. Thus, it is possible to have two estimates of the relative information content of the interferometric systems: according to formula (9) for weak sources and according to the number of cells covered for strong ones (see below).

3. Results of the Numerical Modeling and Discussion of the Results

3.1. Selection of the Initial Parameters. For the RAKSAS-1 model system, we chose a system (Figure 1a) consisting of a single NRT with geographic coordinates $\varphi = 45^\circ$, $\lambda = 0^\circ$, and a single KRT revolving around the Earth in a circular orbit with the following parameters: altitude of orbit H_0 = 350 km, orbital period T_0 = 92 min, inclination of orbital plane $i = 52^\circ$, longitude of the ascending node $\Omega_0 = 0^\circ$, initial phase $\theta_0 = 0^\circ$.

It is obvious that if the duration of the observation period is $T_o \gg T_0$, the dependence of the resulting coverage of the uv-plane on θ_0 will be weak. For $T_o \geq 24$ h, its dependence on Ω_0 will also be weak. Therefore, the zero values of these parameters are chosen purely formally. As will be demonstrated below, the dependence on Ω_0 appears as a dependence on the difference $\alpha - \Omega_0$. In view of this, the values of Ω_0 were not varied.

During the numerical modeling, we made calculations for situations differing in the position of the observed object in the celestial sphere and the duration of the observation period, as well as the number of frequencies analyzed during multifrequency coverage of the uv-plane. In connection with this, the uv-plane was represented in the form of a mass of cells measuring

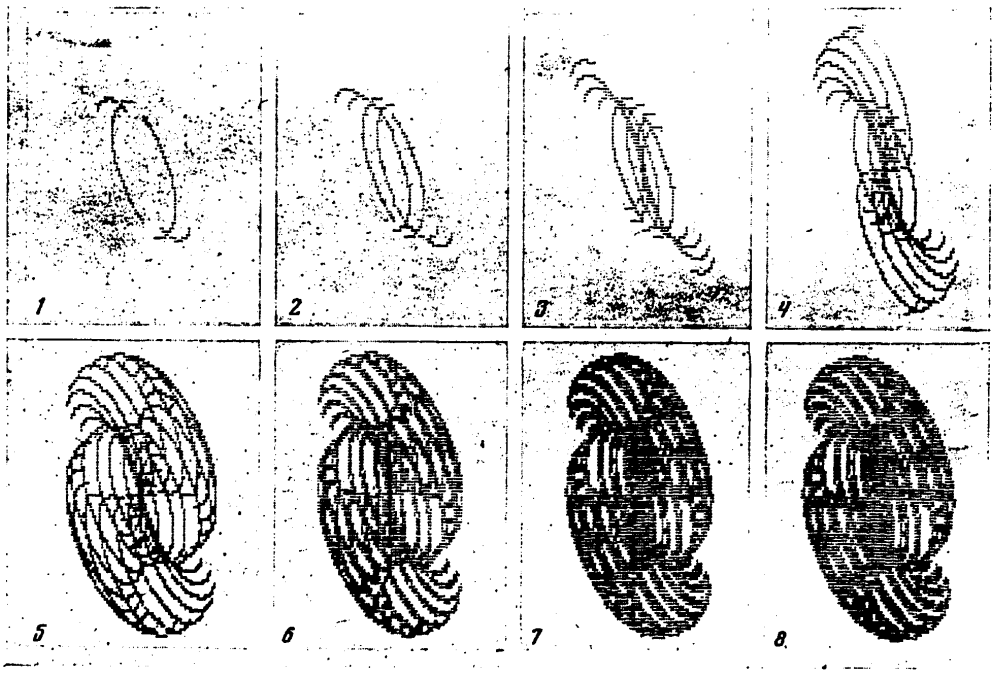

Figure 2. Coverage of uv-plane in the RAKSAS-1 system with $\varphi = 45^\circ$, $\lambda = 0^\circ$, $H_0 = 350$ km, $T_0 = 92$ min, $i = 52^\circ$, $\Omega_0 = 0^\circ$, $\theta = 0^\circ$, $\alpha = 0^h$, $\delta = 45^\circ$, for different observation times: 1.5, 3, 6 and so on, up to 192 h. Division of the uv-plane: 100 x 100 cells.

100 x 100, with the cell having the number (50,50) corresponding to the origin of coordinates, in view of which both halves of the uv-plane are shown in our illustrations, for purposes of clarity.

The linear dimension ΔR of a single cell was chosen from the relationship $50\Delta R = 2R_0$ (where R_0 = radius of the KRT's orbit). This corresponds to a situation where the maximum base realizable by the system, which is $\sim 2R_0$, will be of the size of 50 cells in the discrete representation. Step Δt for the discretization of the process with respect to time was chosen to be 6 s, which corresponds to approximately one-fourth to one-tenth of the average time the projection of the system's base's vector remains in a single cell of the uv-plane during a single pass through it.

3.2. Dynamics of the uv-Plane Coverage Process. Figures 2 and 3 are maps of the coverage of the uv-plane by the RAKSAS-1 system for observed objects

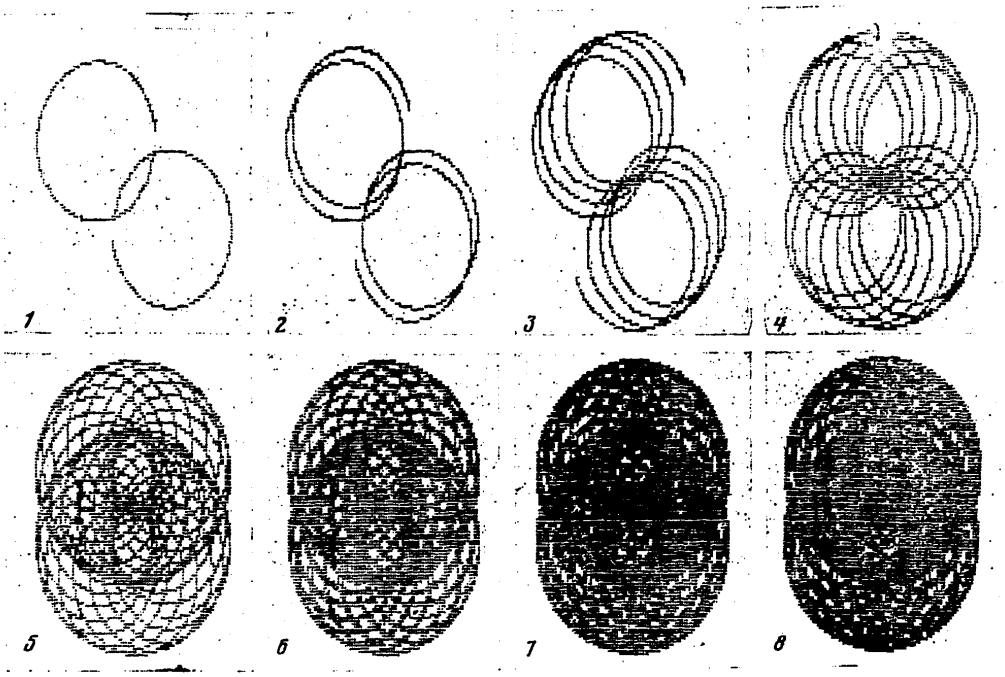

Figure 3. The same as Figure 2, but with $\alpha = 18^h$.

with coordinates $\alpha = 0^h$, $\delta = 45^\circ$ (Figure 2) and $\alpha = 18^h$, $\delta = 45^\circ$ (Figure 3), for different observation period durations T_o. The numbers in the lower lefthand corners of the maps presented here correspond to the total duration of the observation in the following manner:

No	1	2	3	4	5	6	7	8
T_o, h	1.5	3	6	12	24	48	96	192

On the maps corresponding to short periods ($T_o \lesssim 12$ h), the breaks in the tracks of the motion of the projection of the system's base's vector caused by the passing of the KRT into the Earth's shadow, as well as the characteristic epicycloidal nature of the coverage, are quite visible.

Figure 4 depicts the graphs of the dependence of the number of cells covered (in thousands of pieces) on the coverage period's duration T_o. The solid line represents the dependence for a source with coordinates $\alpha = 0^h$, $\delta = 45^\circ$, while the broken line depicts it for one with coordinates $\alpha = 18^h$, $\delta = 45^\circ$. It is obvious that for the given discretization of the uv-plane,

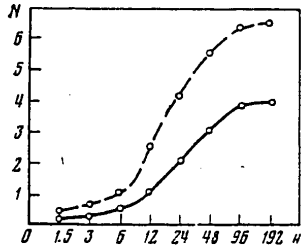

Figure 4. Dependence of the number of covered cells N (in thousands of pieces) in the uv-plane on the duration of source observation, for a 100 x 100 cell layout. Solid line: $\alpha = 0^h$; broken line: $\alpha = 18^h$.

coverage proceeds quite rapidly right up to T_o = 4 days, after which saturation is reached because of the repeated entry of the projection of the system's base's vector into previously covered cells. In connection with this, the coverage factor of a unicompendent area that contains nothing but covered cells is quite high and is 0.5-0.8. Naturally, a reduction in the linear dimensions of the cells or (which is the same thing) an increase in their number in the discrete representation of the uv-plane will reduce the coverage factor and shift the moment when the coverage process reaches saturation toward the longer times.

Precession will change the dynamics of the uv-plane coverage substantially, but only for the longer observation periods. For instance, when the precession rate is 1-2°/day, the linear changes in the base's vector for a characteristic dimension R_0 = 6,700 km will be 200-400 km after 2 days, which corresponds to 1-2 cells for the given discretization. Precession will reduce the degree of overlap of newly covered cells in the peripheral area of the uv-plane and, correspondingly, increase their number, it being the case that this is important for the astrophysical problems solvable with the system and for large base values. When $T_o \leqslant 1$ day, the precession effect cannot have any substantial influence on the coverage.

3.3. Dependence of uv-Plane Coverage on the Observed Object's Coordinates. The data presented in Figures 2-4 indicate that the coverage results depend substantially on the coordinates of the object being investigated. This is related to the fact that at different coordinates, the source will "see" the KRT's orbital plane at different angles. From the viewpoint of completeness of uv-plane coverage, the optimum situation will be that relative positioning of the investigated object and the KRT's orbital plane where vector A of the direction to the object is perpendicular to the orbital plane; in other words, when the orbital plane coincides with the plane of observation. If we look for an extreme with respect to α only, with the other parameters remaining fixed, it will be reached at $\alpha^{(M)} = \Omega_0 - \pi/2$ for $i \leqslant \pi/2$ and $\alpha^{(M)} = \Omega_0 + \pi/2$ for $\pi/2 < i < \pi$, where $\alpha^{(M)}$ is expressed in radians. Because of the influence of the effect of the entry into the Earth's shadow of both the KRT and the NRT, and depending on φ and λ, the value of $\alpha^{(M)}$ giving the maximum number of covered cells in the uv-plane for an orbit with fixed parameters can change slightly relative to the value determined above.

Figure 5 shows maps of uv-plane coverage in 24 h for objects with $\alpha = 0^h$ and δ values that are related to the map number in the following manner:

No	1	2	3	4	5	6	7	8
δ	0°	13°	26°	39°	51°	64°	77°	90°

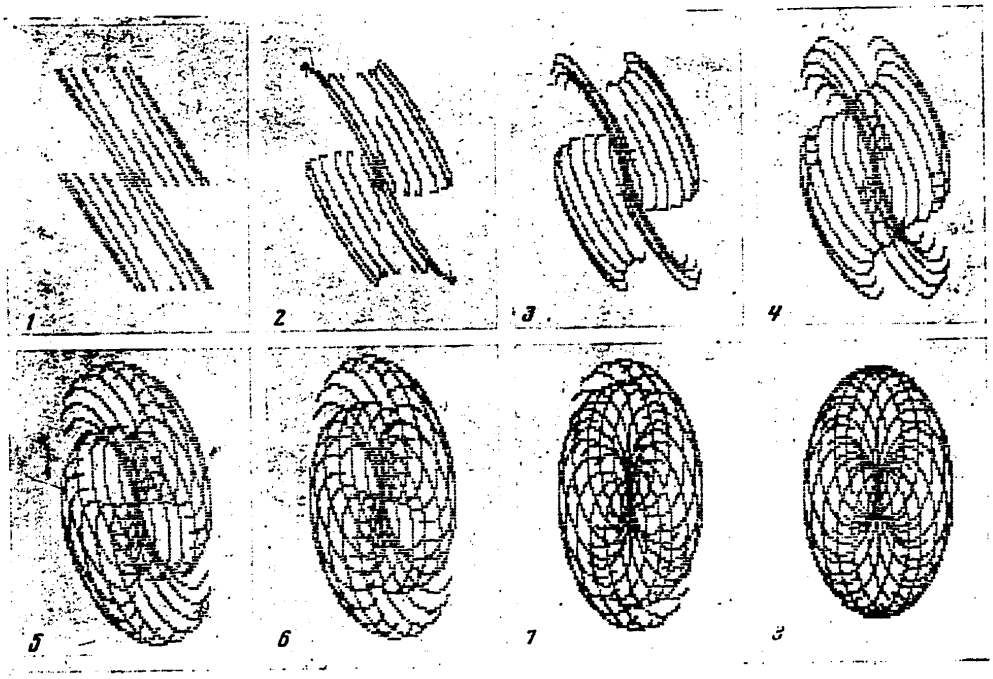

Figure 5. Coverage of the uv-plane in the RAKSAS-1 system for different source declinations (δ = 0°, 13°, 26°, 39°, 51°, 64°, 77°, 90°). Observation time = 24 h; right ascension = 0^h.

Figure 6 shows maps of uv-plane coverage for 24 h for objects with δ = 45° and α values that are related to the map number in the following manner:

No	1	2	3	4	5	6	7	8
α	0^h	3^h	6^h	9^h	12^h	15^h	18^h	21^h

The graph presented in Figure 7a shows the dependence of the number of covered cells in the uv-plane (in thousands of pieces) on the investigated object's right ascension for δ = 45°, T_0 = 24 h. The clear maximum at $\alpha = 18^h$ corresponds to the case where a source with a fixed δ will "see" the orbital plane at the maximum angle. This fact is of considerable importance for selecting the sequence of observation for several objects, since the presence of precession of the orbital plane can, in principle, make it possible to select for each object that moment t_0 for the beginning of observation when the coverage of the uv-plane will be the maximum possible for that object. This, in turn, will make it possible to increase the effectiveness of the observations.

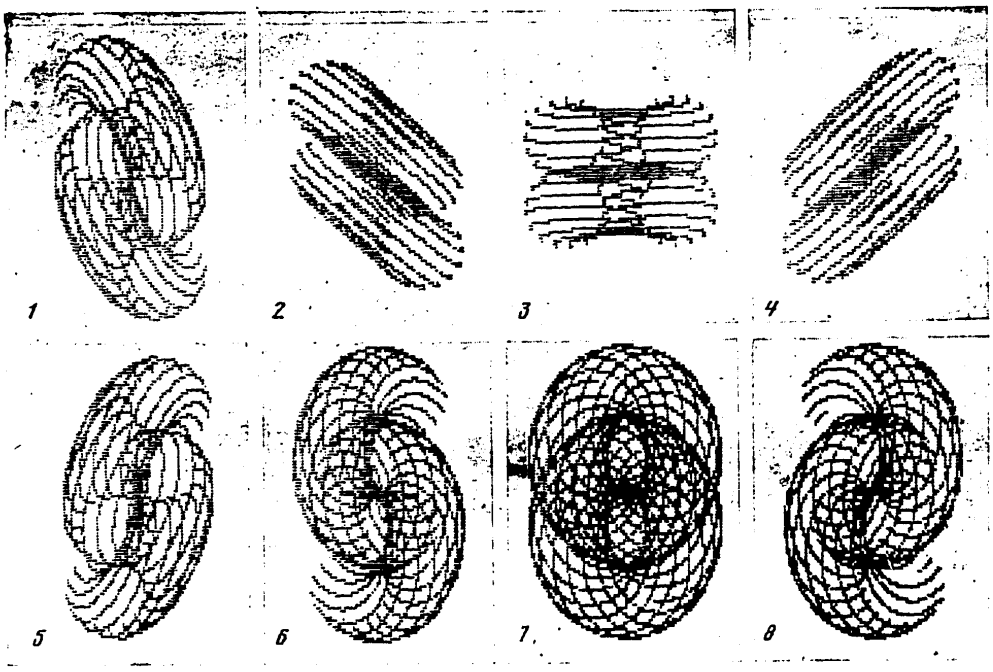

Figure 6. Coverage of the uv-plane in the RAKSAS-1 system for different source right ascensions (α = 0^h, 3^h, 6^h, 9^h, 12^h, 15^h, 18^h, 21^h). Declination = 45°; observation time = 24 h.

The optimum moment for the beginning of observations of a given object can be determined from the relationship

$$\Omega_0(t_0)-\pi/2=\alpha. \qquad (10)$$

It is sufficient to determine the value of t_0 with a degree of accuracy of only several days, because during such a period the effect of orbital precession on the uv-plane coverage process is not substantial.

If a source is observed not only with the optimum right ascension value, but also with the optimum value of declination δ_0, then -- in addition to maximum coverage of the spatial frequency spectrum -- there will be a minimum signal interference frequency. Actually, in this case the projection of the KRT's velocity on the vector A of the direction to the object will be zero and, consequently, the change in the geometric lag (and, from this, the interference frequency) will be determined only by the ground-based telescope's rate of motion.

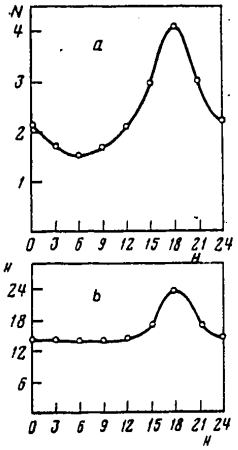

Figure 7. Dependence of the number of covered cells N (in thousands of pieces) in the uv-plane (a) and net synthesis time (b) on the right ascension of a radio source. Declination = 45°; total observation time = 24 h.

In practice, there will be some range of declination angles in which the projection of the KRT's velocity on vector A is sufficiently small; for example, it will not exceed the relative rate of motion of the radiotelescopes in a system of the RSDB type with a base equal to the diameter of the Earth. It is not difficult to demonstrate (see /10/) that the range of declinations for which the indicated condition is fulfilled is $\Delta\delta = \pm 7^{\circ}$ (for the optimum value of α). In connection with this, it is obvious that the interference frequency for RAKSAS-1 will be no greater than for observations with an RSDB system with a base that is close in size to the Earth's diameter. Consequently, in this case the requirements for high operating speed and the range of indeterminacy selection for the frequency's Doppler shift will be the same for observations in RAKSAS-1 as for a ground-based system. Besides this, an important consequence of the choice of the optimum mutual orientation of the investigated source and the KRT's orbital plane is the fact that errors in determining the KRT's coordinates and velocity, which are related primarily to the indeterminacy of its position along the orbit, will enter the analysis with the weighting factor sin $\Delta\delta$; that is, their effect will be reduced substantially.

From the viewpoint of the effectiveness of the observations, one important factor is the net synthesis time; that is, that part of the total observation time during which simultaneous visibility of the investigated source by both radiotelescopes in the system is realized. Figure 7b shows the dependence of net synthesis time T_c on an investigated object's right ascension for $\delta = 45^{\circ}$ and a total observation time $T_o = 24$ h. It is obvious that for the optimum (from the viewpoint of completeness of uv-plane coverage) value $\alpha = 18^h$, the maximum net synthesis time is also realized.

3.4. Distribution of the Number of Covered uv-Plane Cells With Respect to Accumulation Time. For the uv-plane cell coverage algorithm that we have adopted, the accumulation times for a single cell differ. This is related, in the first place, to the nonuniformity of the movement of the projection of the system's base's vector on the uv-plane and, in the second place, to the repeated entries of the projections of the base's vector into already covered cells, which occurs most often for small values of the current base.

During the course of the computations, we constructed the function of the distribution of the number of covered cells with respect to accumulation time for a single cell for the parameters T_0 = 24 h, investigated object coordinates $\alpha = 18^h$, $\delta = 45^o$, and uv-plane division into 100 x 100 cells. When the number of cells in the discrete representation of the uv-plane is increased, the distribution function's maximum is manifested more clearly (see /10/).

The percentage of points with an accumulation time of less than 50 percent of the average time (which is ~40 s for the indicated division) is small (~10 percent) and decreases when the number of cells in the uv-plan division is increased. The range of the change in accumulation time for a single cell is 1-2 orders for a single coverage realization; however, such a broad range is primarily the result of the presence of cells with a very high accumulation time and, as a rule, there are very few of them. It is worth mentioning here that cells with a high accumulation time can be used for the purpose of calibrating the system and for precise phase correlations when solving problems in radioastronomy.

3.5. Comparison With Ground-based Systems of the VLBI and VLBA Type. In order to compare uv-plane coverage by the RAKSAS-1 system with the coverage created by ground-based aperture synthesis systems using the Earth's rotation, two radiointerferometer systems were selected:

a) a two-element type RSDB (VLBI) system with antennas having the geographic coordinates listed in Table 1, which corresponds approximately to a (Simenz-Khaystek) interferometer;

b) the GRT (VLBA) system proposed in /12/, which consists of 10 radiotelescopes having the geographic coordinates listed in Table 2.

Table 1.

Antenna	Latitude	Longitude
1	42.5°	-80.0°
2	44.5°	34.0°

Table 2

Antenna	Latitude	Longitude
1	40.4°	-3.2°
2	38.4°	-77.2°
3	38.5°	-79.8°
4	38.5°	-81.5°
5	38.5°	-85.5°
6	38.5°	-88.0°
7	38.5°	-99.5°
8	38.5°	-111.0°
9	38.5°	-122.4°
10	19.8°	-155.5°

In the calculations it was assumed that the dimensions of all the antennas in the RAKSAS-1, VLBI and VLBA systems were identical. The maps of the uv-plane for each system were reduced to a single scale, so they can be compared to each other directly (keeping in mind the fact that the number of antennas participating in the work of the VLBA system exceeds the number of antennas in the RAKSAS-1 and VLBI systems by a considerable number).

Figure 8 contains maps of the coverage of the uv-plane by the VLBI (top), VLBA (middle) and RAKSAS-1 (bottom) systems, for objects with declinations that correspond to the map number in the following manner:

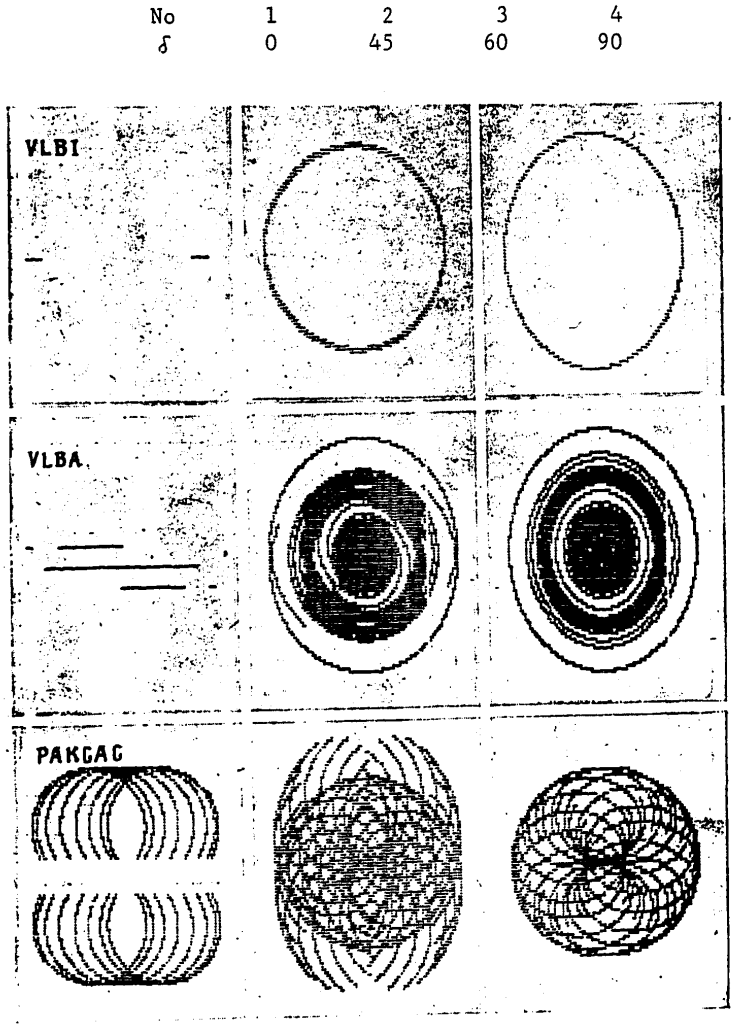

Figure 8. Comparison of uv-plane coverage by different interferometric systems having superlong bases: top row = RSDB (VLBI), 2 ground-based radiotelescopes; middle row = GRT (VLBA), 10 ground-based radiotelescopes; bottom row = RAKSAS-1, 1 space-borne and 1 ground-based radiotelescope. Source declination = 0°, 60°, 90° (from left to right); observation time = 24 h.

Table 3. Comparison of Information Content of VLBI, VLBA and RAKSAS-1 Systems

Declination, δ	Information Parameter	System: VLBI, 2 telescopes	System: VLBA, 10 telescopes	System: RAKSAS-1, 2 telescopes
0°	N, cells	14	130	1,600
	S_1	$2.8 \cdot 10^7$	$1.0 \cdot 10^{10}$	$6.6 \cdot 10^9$
	B_{max}, km	7,650	10,600	12,450
45°	N, cells	335	2,300	4,100
	S_1	$2.9 \cdot 10^8$	$5.4 \cdot 10^{10}$	$1.8 \cdot 10^{10}$
	B_{max}, km	7,700	10,700	12,950
60°	N, cells	405	3,000	3,400
	S_1	$3.6 \cdot 10^8$	$7.5 \cdot 10^{10}$	$1.5 \cdot 10^{10}$
	B_{max}, km	7,750	10,650	12.250
90°	N, cells	300	2,900	2,300
	S_1	$3.0 \cdot 10^8$	$7.9 \cdot 10^{10}$	$1.1 \cdot 10^{10}$
	B_{max}, km	7,800	10,500	1.100

For systems of the VLBI and VLBA type, the investigated source's right ascension is unimportant when daily sysnthesis is performed, while for the RAKSAS-1 the value of α was taken to be 18^h in this case (the optimum value according to Figure 7).

In order to compare the results of uv-plane coverage by the VLBI, VLBA and RAKSAS-1 model systems, Table 3 gives rounded values for the number of covered cells N, the relative information content S_1 for a weak signal, and the maximum base B_{max} realized in the given numerical experiment. Let us recall here that the value of N characterizes the information content of a system when a strong source is observed (see Section 2.4). The total observation time is 24 h in each case. Table 3 corresponds to situations for which the maps are presented in Figure 8.

4. Conclusions

Above we compared the information content of the following systems: VLBI (2 ground-based radiotelescopes in the interferometer made, with a superlong base -- RSDB), VLBA (10 ground-based radiotelescopes in the global aperture synthesis mode -- GRT), and RAKSAS-1 (a ground-based and a low-orbital space radiotelescope in the aperture synthesis mode).

The data that were obtained -- the uv-plane coverage maps and the values presented in Table 3, in particular -- make it possible to draw the following conclusions.

1. The coverage of the spatial frequency plane (the uv-plane) provided by the RAKSAS-1 system, which consists of two radiotelescopes (one ground-based

and one space-borne), is much more nearly complete than that provided by a ground-based, two-element, intercontinental radiointerferometer of the VLBI type.

2. The coverage of the uv-plane by the RAKSAS-1 system over a 24-h period is substantially better (on the average) than that provided by multiantenna (up to 10) global interferometric systems, it being the case that when the duration of the observations is extended beyond 24 h, RAKSAS-1 will make it possible to obtain even better coverage, which -- it goes without saying -- is impossible in the VLBA system.

3. In the case of the observation of a weak source for 24 h, the information content (after Shennon) of the RAKSAS-1 system is only one-third that of the VLBA system (10 telescopes), which is obviously the result of the considerable difference in the collecting areas. It is easy to show that the information content of both systems is comparable when the VLBA system is set up in a seven-antenna version. However, such a system will cover only about one-third the number of uv-plane cells that the RAKSAS-1 will.

4. When formulating a time-correlated program of observations for systems of the RAKSAS-1 type, it is necessary to take into consideration the sources' right ascension and the precession of the KRT's orbital plane, for the purpose of obtaining optimum coverage of the spatial frequency spectrum for each source included in the program.

5. The algorithms and program for the numerical modeling of uv-plane coverage that have been described for the RAKSAS-1 system can be used when selecting objects to the investigated and in the formulation of the temporal sequence for their observation in actual experiments with a space radiointerferometer.

The analysis presented above applies to any ground-based/space-borne aperture synthesis systems of the type under discussion, regardless of the wavelength on which the observations are made. It is of interest to discuss the informational possibilities of other variants of ground-based/space-born and purely space-borne interferometers (with different altitudes and types of orbits), but this goes beyond the framework of this article.

BIBLIOGRAPHY

1. Buyakas, V.I., Gvamichava, A.S., Gorshkov, L.A., Dolgopolov, G.A., Danilov, Yu.I., Zakson, M.B., Kardashev, N.S., Klimashin, V.V., Komarov, V.I., Mel'nikov, N.P., Narimanov, G.S., Prilutskiy, O.F., Pshennikov, A.S., Rodin, V.G., Rudakov, V.A., Savin, A.I., Sagdeyev, R.Z., Semenov, Yu.P., Sokolov, A.G., Usyukin, V.I., Feoktistov, K.P., Tsarevskiy, G.S., and Shklovskiy, I.S., KOSMICHESKIYE ISSLEDOVANIYA (Space Research), Vol 16, 1978, p 773.

2. Buyakas, V.I., Gvamichava, A.S., Gorshkov, L.A., Dolgopolov, G.A., Danilov, Yu.I., Zakson, M.B., Kardashev, N.S., Klimashin, V.V., Komarov, V.I., Mel'nikov, N.P., Narimanov, G.S., Prilutskiy, O.F., Pshennikov, A.S., Rodin, V.G., Rudakov, V.A., Savin, A.I., Sagdeyev, R.Z., Semenov, Yu.P., Sokolov, A.G., Usyukin, V.I., Feoktistov, K.P., Tsarevskiy, G.S., and Shklovskiy, I.S., KOSMICHESKIYE ISSLEDOVANIYA, Vol 16, 1978, p 924.

3. Powell, P.V., and Hibbs, A.R., ASTRON. AERONAUT., Vol 15, 1977, p 58.

4. Basler, R.P., Jonson, C.L., and Vondrak, R.R., RADIO SCI., Vol 12, 1977, p 845.

5. Kardashev, N.S., Pariyskiy, Yu.N., and Sokolov, A.G., USPEKHI FIZ. NAUK (Progress of Physical Sciences), Vol 104, 1971, p 328.

6. Kardashev, N.S., Pariyskiy, Yu.N., and Umarbayeva, N.D., IZV. SPETS. ASTROFIZ. OBSERV. AN SSSR (Bulletin of the Special Astrophysical Observatory, USSR Academy of Sciences), Vol 5, 1973, p 16.

7. Fomalont, E., and Rayt, M., GALAKTICHESKAYA I VNEGALAKTICHESKAYA RADIOASTRONOMIYA (Galactic and Extragalactic Radioastronomy, collection of works), Moscow, Izdatel'stvo Mir, 1976.

8. Kogan, L.R., SVERKHDAL'NYAYA INTERFEROMETRIYA KOMPAKTNYKH RADIOISTOCHNIKOV (Superlong-Range Interferometry of Compact Radio Sources), candidate's dissertation, Institute of Space Research, USSR Academy of Sciences, 1972.

9. Yesepkina, N.A., Korol'kov, D.V., and Pariyskiy, Yu.N., RADIOTELESKOPY I RADIOMETRY (Radiotelescopes and Radiometers), Moscow, Izdatel'stvo Nauka, 1973.

10. Kardashev, N.S., Pogrebenko, S.V., and Tsarevskiy, G.S., PREPRINT IN-TA KOSMICHESKIKH ISSLED. AN SSSR (Preprint, Institute of Space Research, USSR Academy of Sciences), No 449, 1978.

11. Aksenov, Ye.P., TEORIYA DVIZHENIYA ISKUSSTVENNYKH SPUTNIKOV ZEMLI (Theory of the Motion of Artificial Earth Satellites), Moscow, Izdatel'stvo Nauka, 1977.

12. Swenson, G.W., and Kellermann, K.I., SCIENCE, Vol 188, 1975, p 1263.

/356-11746/

11746
CSO: 1866

UDC 629.198.3

ON SELECTING TYPES OF LAUNCH VEHICLES FOR THE IMPLEMENTATION OF A SPACE RESEARCH PROGRAM OVER A MINIMUM PERIOD OF TIME

Moscow KOSMICHESKIYE ISSLEDOVANIYA in Russian Vol 18, No 1, Jan-Feb 80 pp 63-70

[Article by V.P. Ofitserov]

[Text] The author discusses methods for solving the problems that arise during the substantiation of the selection of types of launch vehicles for the implementation of a space research program over a minimum period of time, both with and without limitations on the cost of the research program. He discusses the cases of single and multiple use of launch vehicles. In the solution process, he develops and uses an approach based on the concepts of dynamic programming. The algorithms that are derived can be used in automated design systems and for the solution of individual problems.

1. Let us assume that a space research program is given by the vectors $G = (G_1,\ldots,G_k)$ and $m = (m_1,\ldots,m_k)$, where G_i = weight of the i-th KA [spacecraft] and m_i = number of planned launches of a KA of the i-th type ($i = 1,2,\ldots,k$). The components of vector G are ordered by increasing weight. As is shown in [1], the number of types of launch vehicles (RN) planned and manufactured for a given program cannot exceed the number of types of KA's. In order to avoid considerable complications in the description of the algorithms, we will define the group of RN's by the vectors $G_p = (G_{p1},\ldots,G_{pk})$, $n = (n_1,\ldots,n_k)$ and $r = (r_1,\ldots,r_k)$ where G_{pi}, n_i and r_i are, respectively, maximum liftable weight, number of uses and number of RN's of the i-th type ($i = 1,\ldots,k$). In this notation the planning and manufacturing of an RN of the i-th type (with weight G_p) is determined

by the values of n_i and r_i ($n_i = 0$ and $r_i = 0$ if the i-th type of RN will not be designed and manufactured). Thus, having provisionally fixed the maximum possible number of types of RN's by vector $G_p = (G_{p1},\ldots,G_{pk})$, henceforth we will find the optimum RN planning and manufacturing program with the help of the selection of values of the corresponding components of vectors n and r. As is also the case in [1,2], $G_i \leq G_{pi} \leq G_{i+1}$ ($i = 1,\ldots,k-1$) and $G_k \leq G_{pk}$, and an RN with a maximum liftable weight G_{pi} can be used to lift any KA with a weight $G_j \leq G_{pi}$.

In Section 2 we solve the problem of finding vectors n and r that insure the implementation of the research program in the minimum amount of time, providing that we know the mappings

$$\varphi_1\colon (G_p, n)\to t_1,\ \varphi_2\colon (G_p, n, r)\to t_2,\ \varphi_3\colon (G_p, n)\to t_3, \qquad (1)$$

where t_1 = time outlays per unit of weight of the RN's payload, as derived from calculations of the outlays for scientific research work, experimental design work and mastering the production of the given type of RN; t_2 = time outlays per unit of weight of the RN's payload, as determined by the production of a single RN of the given type; t_3 = time outlays per unit of weight of the RN's payload, as determined by the use of an RN of the given type.

In Section 3 we solve the problem of finding vectors n and r that insure the implementation of the research program in the minimum amount of time, providing that the allocated facilities are limited. In connection with this, in addition to mappings (1) we assume the following mappings to be known:

$$\varphi_4\colon (G_p, n)\to\lambda_1,\ \varphi_5\colon (G_p, n, r)\to\lambda_2,\ \varphi_6\colon (G_p, n)\to\lambda_3, \qquad (2)$$

where λ_1 = cost per unit of weight of the RN's payload, as derived from calculations for the cost of the scientific research and experimental design work and the mastering of the production of the given type of RN; λ_2 = cost per unit of weight of the RN's payload, as determined by the expenditures for the production of a single specific RN of the given type; λ_3 = cost per unit of weight of the RN's payload, as determined by the expenditures for a single use of the RN.

In Section 4 we discuss the same problem as in Section 3, but without limitations, and give a brief description of the algorithms.

2. Let us introduce into our discussion the sets

$$X_1=\{0, m_1\}, \quad X_2=\{0, m_2, m_2+m_1\}, \ldots, \quad X_{k-1}=\left\{0, m_{k-1}, \ldots, \sum_{j=1}^{k-1} m_j\right\},$$

$$X_k=\left\{m_k, m_k+m_{k-1}, \ldots, \sum_{j=1}^{k} m_j\right\}.$$

The values of variable $x_i \in X_i$ (i = 1,...,k) show how many KA's can be lifted by an RN of the i-th type. The question of the relationship of the frequency of use and the number of RN's of the i-th type for the lifting of x_i KA's was discussed in [2]:

$$n_i \in N(x_i), \quad r_i = \bar{E}(x_i/n_i), \tag{3}$$

where $N(x_i)=\bigcup_{j=1}^{x_i}\left\{\bar{E}\left(\frac{x_i}{j}\right)\right\} \forall x_i \in X_i$, for x_i = 0 we assume that $N(x_i)$ = $= \{0\}$; $\bar{E}(\alpha) = E(\alpha) + \beta$, $E(\alpha)$ = the integral part of number α, $\beta=\begin{cases}1, & E(\alpha)\neq\alpha\\ 0, & E(\alpha)=\alpha\end{cases}$, and for n_i = 0 we assume that r_i = 0 (i = $= 1,\ldots,k$).

Using (1), we can determine the time outlays for the development, production and launching of RN's defined by G_{pi}, n_i and r_i:

$$\tilde{g}_i=[t_1(G_{p_i}, n_i)+t_2(G_{p_i}, n_i, r_i)r_i+t_3(G_{p_i}, n_i)]G_{p_i} \quad (i=1,\ldots).$$

Taking (3) into consideration, $\tilde{g}_i = \tilde{g}_i(n_i, x_i)$ for a given G_{pi}. We will assume that $\tilde{g}_i(0, x_i) = +\infty$ for $x_i \neq 0$, while $\tilde{g}(0,0) = 0$.

In order that the program of launches of the first ℓ types of KA's be implemented in the minimum period of time, it is necessary that these conditions be fulfilled:

$$x_i \in X_i \ (i=1,\ldots,l), \qquad x_1+x_2+\ldots+x_l=\sum_{j=1}^{l} m_i, \tag{4a}$$

$$\forall i \exists \gamma \quad x_\gamma \geqslant \sum_{j=i}^{\gamma} m_j (i \in \{1,\ldots,l\}, \ \gamma \in \{i, i+1, \ldots, l\}), \tag{4b}$$

$$n_i \in N(x_i), \quad r_i = \bar{E}\left(\frac{x_i}{n}\right), \tag{4c}$$

where (ℓ = 1,2,...,k).

Actually, conditions (4b) and (4c) guarantee the launching of KA's of the first ℓ types, while conditions (4a) and (4c)

exclude the creation of a group of RN's designed for the launching of a larger number of KA's than is given in the program.

Example. Let $G = (G_1,G_2,G_3)$, $m = (m_1,m_2,m_3 = (2,2,2)$. The group of RN's will then consist of no more than three types; that is, $G_p = (G_{p1},G_{p2}, G_{p3})$, while each type of RN can lift into orbit KA's from the respective sets $X_1 = \{0,2\}$, $X_2 = \{0,2,4\}$, $X_3 = \{2,4,6\}$. Condition (4a) insures the launching of six KA's $\left(\sum_{j=1}^{3} m_j=6=\sum_{i=1}^{3} x_i,\ x_i\in X_i\right)$. However, it is possible to have a variant where $x_1 = 0$, $x_2 = 2$, $x_3 = 4$; that is, (4a) is fulfilled, but providing that there exists an RN of type $G_{p2} < G_{p3}$, a KA of type G_1 will be lifted by an RN of type G_{p3} or an RN of type G_{p2} (in the latter case, a KA of type G_2 is lifted by an RN of type G_{p3} when there is an RN of type G_{p2}), which is not the optimum solution with respect to either time of implementation of the program or its cost. Such variants are eliminated by condition (4b). Actually, in this case for $i = 1$ we cannot find a value of γ so that $x_1\geqslant\sum_{j=1}^{\gamma} m_j$, $\gamma\in\{1,2,3\}$. On the other hand, the values $x_1 = 2$, $x_2 = 4$, $x_3 = 6$ satisfy (4b), but the RN system will be designed for 12 launches, which is just as nonoptimal. Similar variants are eliminated by condition (4a). For values of x_i satisfying (4a) and (4b), conditions (4c) give the possible values of n_i and the corresponding values of r_i, and in connection with this eliminate the known nonoptimal values. For instance, for $x_1 = 0$, $x_2 = 4$, $x_3 = 2$, from (4c) we obtain:

$$n_1=0,\quad r_1=0;\quad n_2\in N(4)=\bigcup_{j=1}^{4}\left\{E\left(\frac{4}{j}\right)\right\}=\{4,2,1\},\quad r_2=E\left(\frac{4}{n_2}\right);$$

$$n_3\in N(2)=\{2,1\},\quad r_3=E\left(\frac{2}{n_3}\right).$$

For each $x_i\in X_i$ ($i = 1,\ldots,k$), we determine

$$g_i(x_i)=\min_{n_i\in N(x_i)}\tilde{r}(n_i,x_i) \tag{5}$$

and remember the values of n_i that give $g_i(x_i)$.

Now, in order to determine the group of RN's for the implementation of the program in the minimum amount of time, let us examine the recurrent relation

$$f_l\left(\sum_{j=1}^{l} m_j\right) = \min_{x_l \in X_l}\left[g_l(x_l) + f_\alpha\left(\sum_{j=1}^{l} m_j - x_l\right)\right], \quad (l=2,3,\ldots,k). \tag{6}$$

The value of α is determined from the condition $\sum_{j=1}^{\alpha} m_j = \sum_{j=1}^{l} m_j - x_l$

(for $\sum_{j=1}^{l} m_j - x_l = 0$ we assume that $f_\alpha(0) = 0, \alpha = 0$), $f_1(m_1) = g_1(m_1), \; x_l \neq 0$.

Let us mention here that in view of the existence of recurrent relation (6), conditions (4) are automatically fulfilled and, consequently, all the values of variables x_l for which an optimum solution can be achieved will be taken into consideration.

Relationship (6) is nothing other than the basic functional equation of dynamic programming [3] as applied to this problem, so that $f_k\left(\sum_{j=1}^{k} m_j\right)$ will be the minimum time for implementation of the program. A more detailed substantiation of the applicability of the dynamic programming method to problems of selecting groups of RN's can be found in [1,2]. In contrast to [1,2], in this article the functional equation is derived in explicit form.

For values of x_l yielding $f_k\left(\sum_{j=1}^{k} m_j\right)$, from (5) we find the appropriate values of n_l, while from (3) we determine r_l for x_l and n_l and assume that the other values of n_l and r_l equal zero.

Example. Let $G = (G_1, G_2, G_3)$ and $m = (2,2,2)$. It is then the case that $G_p = (G_{p1}, G_{p2}, G_{p3})$. It is necessary to find $n = (n_1, n_2, n_3)$ and $r = (r_1, r_2, r_3)$ on condition that the program of launches is implemented in the minimum time. From (5) we find that $g_i(0) = 0$ $(i = 1,2,3)$ and $g_i(2) = \min_{n_i \in \{2,1\}} \bar{g}_i(n_i, 2)$. We determine the other values of $g_i(x_i)$ analogously. Let us assume

that $g_1(2) = \tilde{g}_1(1,2)$, $n_1 = 1$; $g_2(2) = \tilde{g}_2(2,2)$, $n_2 = 2$; $g_2(4) = \tilde{g}_2(4,4)$, $n_2 = 4$; $g_3(2) = \tilde{g}_3(2,2)$, $n_3 = 2$; $g_3(4) = \tilde{g}_3(1,4)$, $n_3 = 1$; $g_3(6) = \tilde{g}_3(6,6)$, $n_3 = 6$.

Assuming that $\ell = 2, 3$ in (6), we find $f_1(2) = g_1(2)$, $f_2(4)$, $f_3(6)$. Let us assume that $f_3(6) = g_3(2) + f_2(4) = g_3(2) + g_2(4)$. Above we found the values of n_i for each $g_i(x_i)$. Using this, let us obtain the optimal solution for $x_3 = 2$, $x_2 = 4$, $n_3 = 2$, $n_2 = 4$, $n_1 = 0$, $r_3 = \bar{E}(2/2) = 1$, $r_2 = 1$, $r_1 = 0$. Thus, $n = (0,4,2)$, $r = (0,1,1)$ and an RN of type G_{p1} does not work out.

The results that have been obtained can easily be extended to the cases of different limitations on the types of RN's and frequency of use or number of RN's of each type. Moreover, the algorithm works more effectively if, for example, n_i cannot take on all the values from $N(x_i)$ but only some of them, since this makes it possible to determine $g_i(x_i)$ from (5) more rapidly. Actually, if we assume that $n_3 \in \{1,2\}$ in the preceding example, the computations of $g_3(x_3)$ are simplified.

If limitations are imposed on r_i ($r_i \in R_i$), the set $N(x_i)$ is defined in the following manner:

$$N(x_i)=\left\{n_i | n_i=E\left(\frac{x_i}{r_i}\right), x_i \in X_i, \forall r_i \in R_i\right\}, \qquad (7)$$

where for $r_i = 0$ we assume that $n_i = 0$ ($i = 1,\ldots,k$), and the solution algorithm does not change after the appropriate sets are replaced.

Let us make special note of the fact that in the case of a single RN use, $\forall x_i \in X_i N(x_i) \subset \{0,1\}$, while in the case where several RN's cannot be developed, we assume that the corresponding $N(x_i) = \{0\}$.

It is also necessary to mention that in the solution of the problem we did not take into consideration the actual time for the execution of the research that is not related to the development and production of RN's, so that -- speaking more rigorously -- the value of $f_k\left(\sum_{j=1}^{k} m_j\right)$ found from (6) is only the criterion for determining the group of RN's that, however, actually implement the research program in the minimum time.

3. Let us assume that the means allocated for the space research program are limited and that their value does not exceed C*. Using (2), it is possible to determine the cost of the development, production and launching of the RN's defined by G_{pi}, n_i, r_i (i = 1,...,k):

$$\tilde{h}_i=[\lambda_1(G_{p_i}, n_i)+\lambda_2(G_{p_i}, n_i, r_i)r_i+\lambda_3(G_{p_i}, n_i)]G_{p_i}.$$

Taking (3) into consideration, $\tilde{h}_i = \tilde{h}_i(n_i,x_i)$ for a given G_{pi}. We will assume that $\tilde{h}_i(0,x_i) = +\infty$ for $x_i \neq 0$, while $\tilde{h}_i(0,0) = 0$. For each $x_i \in X_i$ (i = 1,...,k) let us determine

$$h_i(x_i)=\min_{n_i \in N(x_i)} \tilde{h}_i(n_i, x_i) \tag{8}$$

and remember the values of n_i that give $h_i(x_i)$.

Let us examine the process of finding the group of RN's for the implementation of the program in the minimum time, given a limited program cost, in steps.

Step 1. Let us determine the group of RN's that implements the launch program of the first l types of KA's with a minimum cost, using the recurrent relation

$$w_l\left(\sum_{j=1}^{l} m_j\right)=\min_{x_l \leq x_l}\left[h_l(x_l)+w_\alpha\left(\sum_{j=1}^{\alpha} m_j-x_l\right)\right], \tag{9}$$

where l = 2,3,...,k; α is determined from the condition

$\sum_{j=1}^{\alpha} m_j=\sum_{j=1}^{l} m_j-x_l$ (for $\sum_{j=1}^{l} m_j-x_l=0$ we assume that $w_\alpha(0) = 0$, $\alpha = 0$), $w_1(m_1) = h_1(m_1)$, $x \neq 0$.

As was the case with (6), here condition (4) is fullfilled automatically. If $w_k\left(\sum_{j=1}^{k} m_j\right)>C^*$, the problem does not have a solution. Let $w_k\left(\sum_{j=1}^{k} m_j\right)\leq C^*$. Let us designate as X_k^1 the set of values x_k such that

$$h_k(x_k)+w_\alpha\left(\sum_{j=1}^{k} m_j-x_k\right)\leq C^*, \tag{10}$$

that is,

$$X_k' = \{x_k | h_k(x_k) + w_\alpha \left(\sum_{j=1}^{k} m_j - x_k \right) \leq C^*, \; x_k \in X_k \},$$

where α is determined from the condition $\sum_{j=1}^{\alpha} m_j = \sum_{j=1}^{k} m_j - x_k$, and for $x_k = \sum_{j=1} m_j$ we assume that $\alpha = 0$, $w_\alpha = 0$.

The solution of the problem can obviously exist only for $x_k \in X_k'$, because otherwise the program's cost will be more than C*. From among the groups of RN's determined by (9) for each $x_k \in X_k'$, we select the one to which the minimum time corresponds. Let us designate this time as $t(w_k)$.

Let X_k'' be the set of values of x_k such that

$$g_k(x_k) + f_\alpha \left(\sum_{j=1}^{k} m_j - x_k \right) \leq t(w_k), \; x_k \in X_k', \tag{11}$$

that is,

$$X_k'' = \left\{ x_k | g(x_k) + f_\alpha \left(\sum_{j=1}^{k} m_j - x_k \right) \leq t(w_k), \quad x_k \in X_k' \right\},$$

where α is determined as it was previously.

It is obvious that $X_k'' \subset X_k' \subset X_k$ and the solution of the problem can be improved only for $x_k \in X_k''$, because otherwise either the time evaluation will be greater than $t(w_k)$ or the cost evaluation will be greater than C*.

If among the groups of RN's determined by (6) for each $x_k \in X_k''$ are found those not costing more than C*, we select the group of RN's to which the minimum time corresponds and call this time $t(f_k)$ (let it be noted that $t(f_k) \leq t(w_k)$). Otherwise, the time evaluation is kept as $t(w_k)$.

Let us define as $\bar{x}_k$ the value of $x_k \in X_k''$ that corresponds to the group of RN's with time $t(w_k)$ ($t(f_k)$, if the corresponding group of RN's exists).

Although all the other steps of the algorithm differ from the first one, they do not differ from each other, so we will now describe some step P.

Step P. Having eliminated $\bar{x}_{\alpha_1}$ from X''_{α_1}, let us turn to a discussion of the launch program of the first α_{i+1} types of KA's, where α_{i+1} is determined from the relationship $\sum_{j=1}^{\alpha_{i+1}} m_j = \sum_{j=1}^{\alpha_i} m_j - \bar{x}_{\alpha_i}$; for $\bar{x}_{\alpha_i} = \sum_{j=1}^{\alpha_i} m_j$ we assume that $\alpha_{i+1} = 0$, $X_{\alpha_{i+1}} = \emptyset$.

In order to improve the solution, it is necessary to implement this program in accordance with conditions (12), which determine the set $X''_{\alpha_{i+1}}$:

$$h_{\alpha_{i+1}}(x_{\alpha_{i+1}}) + w_{\alpha_{i+2}}\left(\sum_{j=1}^{\alpha_{i+1}} m_j - x_{\alpha_{i+1}}\right) \leqslant$$

$$\leqslant c' - \bar{h}_k(n_k, \bar{x}_k) - \bar{h}_\alpha(n_\alpha, \bar{x}_\alpha) - \ldots - \bar{h}_{\alpha_i}(n_{\alpha_i}, \bar{x}_{\alpha_i}), \qquad (12a)$$

$$g_{\alpha_{i+1}}(x_{\alpha_{i+1}}) + f_{\alpha_{i+2}}\left(\sum_{j=1}^{\alpha_{i+1}} m_j - x_{\alpha_{i+1}}\right) \leqslant$$

$$\leqslant t' - \tilde{g}_k(n_k, \bar{x}_k) - \tilde{g}_\alpha(n_\alpha, \bar{x}_\alpha) - \ldots - \tilde{g}_{\alpha_i}(n_{\alpha_i}, \bar{x}_{\alpha_i}), \qquad (12b)$$

where $x_{\alpha_{i+1}} \neq 0$, while α_{i+2} is found from the relationship $\sum_{j=1}^{\alpha_{i+2}} m_j = \sum_{j=1}^{\alpha_{i+1}} m_j - x_{\alpha_{i+1}}$ and for $x_{\alpha_{i+1}} = \sum_{j=1}^{\alpha_{i+1}} m_j$ we assume that $\alpha_{i+2} = 0$, $X_{\alpha_{i+2}} = \emptyset$; t^* = minimum estimate of time for implementation of the entire program, $\tilde{h}_{\alpha_i}(n_{\alpha_i}, \bar{x}_{\alpha_i})$, $\tilde{g}_{\alpha_i}(n_{\alpha_i}, \bar{x}_{\alpha_i})$ show the cost and time, respectively, needed for the development and production of RN's of type α_i, for lifting $\bar{x}_{\alpha_i}$ KA's, with a frequency of use n_{α_i}, as found earlier when determining specific groups of RN's.

A. Let $X''_{\alpha_{i+1}} \neq \emptyset$, so that:

1) if among the groups of RN's determined by (6) for each $x_{\alpha_{i+1}} \in X''_{\alpha_{i+1}}$ we find some that cost no more than the right side of (12a), from among them we select the group of RN's to which

the minimum time $t(f_{\alpha_{i+1}})$ corresponds and designate the corresponding $x_{\alpha_{i+1}}$ as $\bar{x}_{\alpha_{i+1}}$; by doing this we obtain a new estimate of the time for the implementation of the entire program:

$$t'=t(f_{\alpha_{i+1}})+\tilde{g}_{\alpha_i}(n_{\alpha_i},\bar{x}_{\alpha_i})+\tilde{g}_{\alpha_{i-1}}(n_{\alpha_{i-1}}\bar{x}_{\alpha_{i-1}})+\ldots+\tilde{g}_k(n_k,\bar{x}_k)$$

and move on to step P + 1; if we do not find such groups of RN's, we move on to Paragraph 2;

2) if among the groups of RN's determined by (9) for each $x_{\alpha_{i+1}}\in X''_{\alpha_{i+1}}$ we find some to which correspond a time less than the right side of (12b), we select from among them the group of RN's to which the minimum time $t(w_{\alpha_{i+1}})$ corresponds and designate the corresponding $x_{\alpha_{i+1}}$ and $\bar{x}_{\alpha_{i+1}}$; by doing this we obtain a new estimate of the time for the implementation of the entire program:

$$t'=t(w_{\alpha_{i+1}})+\tilde{g}_{\alpha_i}(n_{\alpha_i},\bar{x}_{\alpha_i})+\tilde{g}_{\alpha_{i-1}}(n_{\alpha_{i-1}},\bar{x}_{\alpha_{i-1}})+\ldots+\tilde{g}_k(n_k,\bar{x}_k)$$

and move on to step P + 1; if we do not find such groups of RN's, we move on to Paragraph 3;

3) we select an arbitrary $x_{\alpha_{i+1}}\neq 0$, $x_{\alpha_{i+1}}\in X''_{i+1}$, designate it as $\bar{x}_{\alpha_{i+1}}$ and move on to step P + 1.

B. Let $X''_{\alpha_{i+1}}=\emptyset$, and we then look for the set X''_{α_j} with a minimum index α_j $(j<i+1)$ (let us remember that $\alpha_{i+1}<\alpha_i<\ldots<\alpha_1<<\alpha<k$) that contains elements satisfying (12) for the last estimate of t*, while elements not satisfying (12) are deleted;

a) if such a set X''_{α_j} is found, we select an arbitrary $x_{\alpha_j}\in X''_{\alpha_j}$, designate it as $\bar{x}_{\alpha_{i+1}}$ and move on to step P + 1;

b) if no such set X''_{α_j} is found, the process is ended; t* = minimum time of implementation of the program given a limitation on its cost. Step P + 1 differs from Step P by the change in the indices.

In order to determine the group of RN's that solve the problem, for each estimate of t* that is obtained it is necessary to recall the set $\bar{x}_i$ and the corresponding values of n_i. The set $\bar{x}_i$ and n_i yield the last estimate of t* and the unknown group of RN's will be determined.

Since the sets X_i $(i=1,\ldots,k)$ are finite and from the discussion we have eliminated only those variants that do not improve the solution, we can conclude that the algorithm is finite and yields the optimum solution for the given limitations.

As was the case in Section 2, the results that have been obtained are easily extended to cases of different limitations on n and r (see Section 2).

Example. As before, let $G = (G_1, G_2, G_3)$ and $m = (2,2,2)$.

It is necessary to find n and r that determine the group of RN's for the implementation of the KA launching program over a minimum period of time and with limitations on the cost.

Step 1. Using (9), we determine the group of RN's that implements the KA launching program with the minimum cost. Let us assume that the minimum cost is obtained for $x_3 = 6$, $n_3 = 6$, $r_3 = 1$, $n_1 = n_2 = 0$, $r_1 = r_2 = 0$; that is, the group of RN's is determined by $n = (0,0,6)$, $r = (0,0,1)$ (an RN of the type G_{p3} is developed and produced, with a frequency of use $n_3 = 6$ and in the amount $r_3 = 1$).

If $w_3(6) > C^*$, the problem cannot be solved. Let $w_3(6) \leqslant C^*$ and $X_3' = \{6,4\}$; that is, for $x_3 = 2$ condition (10) is not fulfilled (this means that any group in which an RN of the G_{p3} type lifts two KA's does not satisfy the cost limitation). From among the groups of RN's determined by (9) for each $x_3 \in \{6,4\}$, we select the one to which the minimum time corresponds. Let this be the group corresponding to $x_3 = 4$: $n = (2,0,4)$, $r = (1,0,1)$. Let us designate the time value obtained as $t(w_3)$ ($t(w_3) = \tilde{g}_1(2,2) + \tilde{g}_3(4,4)$). We will check condition (11) for $x_3 \in \{6,4\}$. For $x_3 = 6$, let the RN system that is temporally optimal (in the general case it is different from the one obtained above for $x_3 = 6$ and the minimum cost criterion) yield a time evaluation $g_3(6) > t(w_3)$. It is then the case that $X_3'' = \{4\}$. Let us assume that for $x_3 = 4$, the RN system $n = (1,0,1)$, $r = (2,0,4)$, as found according to the minimum time criterion (by (6)), does not satisfy the cost limitation; that is,

$$\tilde{h}_1(1,2) + \tilde{h}_3(1,4) > C^*.$$

The time evaluation will then by kept as $t(w_3)$. Let us designate x_3 as $\bar{x}_3$ and remember $n_3 = 4$.

Step 2. Let us eliminate $\bar{x}_3 = 4$ from X_3'' and discuss the launch program of the first α types of KA's; we determine α from the relationship

$$\sum_{j=1}^{\alpha} m_j = \sum_{j=1}^{3} m_j - 4 = 6 - 4 = 2 = m_{i_1},$$

that is, $\alpha = 1$. Let us examine $X_1 = \{0,2\}$. For $x_1 = 2$, conditions (12) are

$$h_1(2) \leq C^* - \tilde{h}_3(4,4), \quad g_1(2) \leq t^* - \tilde{g}_3(4,4)$$

and are fulfilled, since $h_1(2) \leq \tilde{h}_1(2,2)$, $\tilde{h}_1(2,2) + \tilde{h}_3(4,4) \leq C^*$; $g_1(2) \leq \tilde{g}_1(2,2)$, $t^* = t(w_3) = \tilde{g}_1(2,2) + \tilde{g}_3(4,4)$. This means that $X_1'' = \{2\}$. For $x_1 = 2$, let the group of RN's G_{p1}, $n_1 = 1$, $r_1 = 2$, as determined by the minimum time criterion, cost no more than $C^* - \tilde{h}_3(4,4)$; that is, $\tilde{h}_1(1,2) \leq C^* - \tilde{h}_3(4,4)$. The time evaluation will then be improved and will equal

$$t' = t(f_1) + \tilde{g}_3(4,4) = g_1(2) + \tilde{g}_3(4,4) = \tilde{g}_1(1,2) + \tilde{g}_3(4,4).$$

Let us designate x_1 as $\bar{x}_1$ and remember that $n_1 = 1$.

Step 3. We eliminate $\bar{x}_1 = 2$ from X_1''. We have $X_0'' = X_1'' = X_3'' = \emptyset$. Consequently, the process is completed. The solution of the problem is obtained for $\bar{x}_3 = 4$, $n_3 = 4$, $\bar{x}_1 = 2$, $n_1 = 1$. From (3) we find $r_3 = 1$, $r_1 = 2$. Thus, for the implementation of the launch program over the minimum period of time, with a cost limitation, it is necessary to develop and produce RN's of type G_{p1} with frequency of use $n_1 = 1$ in the quantity $r_1 = 2$, and an RN of type G_{p3} with frequency of use $n_3 = 4$ in the quantity $r_3 = 1$.

4. The algorithm explained in Section 3 can, without any substantial changes, be used to solve the problem of selecting a group of RN's for the implementation of the program with minimum cost, providing that the program implementation time is limited. In this case it is necessary to substitute (9) for (6), (10) for (11), (11) for (10), (12a) for (12b), (12b) for (12a), and (6) for (9), and instead of time evaluations obtain evaluations of the cost of implementing the entire program with a time limitation.

If, for each value of $x_i \in X_i$ ($i = 1,2,\ldots,k$) we recall the estimates given by (6) and (9), the solution algorithm for the problem with limitations will be efficient with respect to calculation time on a computer, but may require a significant memory capacity (this depends basically on the dimensionality k of the problem being solved).

If the estimates are computed each time that this is necessary, an insignificant memory capacity is required but the problem solution time increases. Compromise variants are possible.

About the algorithm for solving the problem without limitations, it can be said that it is not sensitive to dimensionality and is efficient as far as calculation time on a computer is concerned.

BIBLIOGRAPHY

1. Sollogub, A.V., and Ofitserov, V.P., KOSMICH. ISSLED. (Space Research), Vol 15, No 6, 1977, p 850.

2. Sollogub, A.V., and Ofitserov, V.P., KOSMICH. ISSLED., Vol 16, No 4, 1978, p 514.

3. Bellman, R., and Dreyfus, S., PRIKLADNYYE ZADACHI DINAMICHESKOGO PROGRAMMIROVANIYA (Applied Problems in Dynamic Programming), Moscow, Izdatel'stvo Nauka, 1965.

[8144/1250-11746]

11746
CSO: 8144/1250

SPACE POLICY AND ADMINISTRATION

UDC 502.3:330.115

SOVIET PERCEPTIONS OF UNITED STATES REMOTE SENSING PROGRAM

Moscow ISSLEDOVANIYE ZEMLI IZ KOSMOSA in Russian No 3, 1980 pp 111-119

[Article by K. Ya. Kondrat'yev, "Prospects for Meteorological Observations from Orbital Space Stations in the United States"]

[Text] Experience in carrying out scientific programs with manned spaceships and orbital space stations in the USSR has convincingly demonstrated the good possibilities for their use in meteorological observations [1-9]. This is determining the further development of this type of investigations. In this connection it is of interest to examine the plans laid in the United States related primarily to the development of methods and apparatus for monitoring climatic parameters and factors, taking into account the specific characteristics of manned flight vehicles: presence of a specialist capable of controlling the complex instrumentation which can be carried aboard an orbital space station, who can make a choice of objects for study, etc.

Very significant possibilities for the monitoring of climate are afforded by the programs for orbital space stations and the reusable transport ship being developed in the United States and also the "Spacelab" manned orbital station which is being created by the European Space Agency in collaboration with the United States [10]. The development of the shuttle began in January 1972 and the planning of the "Spacelab" station, which was to be put into orbit by the shuttle, began in 1973. The task of the shuttle, which has a length of 18 m and a width of 4.5 m [dimensions of cargo bay], includes putting different kinds of freight into orbit, including satellites and manned space stations, carrying out operations for the inspection and repair of space vehicles as well as implementing different scientific research programs. The shuttles are capable of functioning in space from 7 to 30 days.

Implementation of the project as a whole was planned for 1980-1990. The research program for the "Spacelab" orbital space station includes five sections: 1) natural resources; 2) weather and climate; 3) physics of the earth and ocean; 4) technology of materials; 5) communications and

navigation. The goals of investigations of natural resources provide primarily for the monitoring of the parameters of the land and ocean. With respect to the ocean, this involves study of the state and temerature of the surface, waves, sea currents, ice conditions and color of the sea. Practical applications include improvement in weather forecasting, study of fish resources, processes in the coastal zone and contamination of the ocean, as well as support of operations at sea. Investigations of the land will be carried out in the interests of such branches as forestry and agriculture, land use, geology, water resources, etc.

The principal research tools will be multispectral cameras and scanning radiometers, spectrometers, passive and active radar apparatus, laser systems, spectrometers and radiometers for the monitoring of solar radiation. There must be assurance of high spatial and spectral resolution, on-board calibration and compatability of instrument parameters, partial processing of data on board and delivery of some of the data to the earth via the shuttle transport ship. Plans call for synchronous observations with automatic satellites for the purpose of obtaining greater detail and comparison and also surface and aircraft subsatellite observations.

Taking into account the great promise of microwave remote sensing, one of the initial goals of "Spacelab" is a testing of microwave radiometers ensuring a high spatial resolution (about 10-15 km), which requires the deployment of large (tens of meters) antennas, whose installation on automatic satellites for the time being is impossible. This is entirely feasible, however, when using a transport ship. The same applies to the use of radars with a synthesized aperture requiring high power consumption and the transmission of a great volume of data to the earth. Plans call for the installation of a complex of automatic instrumentation aboard the shuttle transport ship for the study of natural resources.

The section devoted to the study of weather and climate provides for achieving the following goals: 1) improvement in weather forecasts on the basis of using data from remote sensing of the atmosphere; 2) monitoring of natural and anthropogenic contaminations of the atmosphere; 3) solution of problems involved in the modification of weather and climate (reference is to the use of remote sensing data for developing models and clarification of the mechanisms explaining possible means for inadvertent and purposeful modification of weather and climate: 4) support of a service for warning about dangerous phenomena; 5) use of data from results of remote sensing of the atmosphere, the results of measurements of the radiation balance of the planet and monitoring of variations of exo-atmospheric solar radiation for studying the complex interaction of processes determining weather and climate.

In connection with solution of the enumerated problems plans call for the use of shuttles and orbital stations for: 1) launching of automatic meteorological satellites (since they are put into polar orbits with an

altitude of 1,000-1,700 km, this will become possible only in 1983-1984, after which ordinary means for the launching of meteorological satellites will go out of use); 2) the carrying out of meteorological experiments abroad a shuttle and orbital stations with the participation of a professional meteorologist; 3) servicing (repair, replacement of instrumentation, etc.) of automatic meteorological satellites, which promises substantial economic advantages.

The complex of instrumentation for investigations in the field of meteorology consists of: instruments for the monitoring of solar activity and remote sensing of the atmosphere; improved multichannel two-polarization microwave radiometer with a large antenna; radiometers for studying clouds; radar-laser systems; apparatus for experimental study of the microphysics of interaction among cloud particles under weightlessness conditions; multichannel scanning radiometer for operation in a geostationary orbit for the purpose of continuous monitoring of dangerous phenomena.

The instrumentation for the monitoring of solar activity (prism monochromator and pyrheliometer) provides for the measurement of the spectral distribution of energy in the exoatmospheric solar spectrum for the wavelength range 0.27-4.0μm with an accuracy better than 5% and the integral solar constant with an accuracy better than 1%. The radiometers for the study of clouds have the purpose of solving problems in determining the altitude of the upper cloud boundary on the basis of absorption in the 0.76-μm oxygen band; identification of phase state from reflectivity at a wavelength of 1.61μm; determination of the numerical concentration of droplets using measurements of cloud brightness in the visible part of the spectrum and emissivity of a wavelength of 11 m; determination of the microstructure (size distribution of particles) using data on outgoing radiation at wavelengths of 11 and 24μm; restoration of the geometrical thickness of clouds on the basis of data on brightness in the visible region of the spectrum and IR radiation at the two mentioned wavelengths.

Appropriate theoretical investigations were undertaken in connection with solution of the enumerated inverse problems. The basic objective of the program for investigation of physics of the earth and ocean is obtaining information necessary for developing models for the prediction of earthquakes, circulation of the ocean and conditions at the ocean surface, and refinement of figure of the geoid. Within the framework of the program for study of the physics of the earth there will be an investigation of the structure and motion of tectonic platforms, movement of faults and dislocations, hidden faults, drift of the poles and rate of the earth's rotation, interaction between the crust and mantle, tides in the earth's crust, spatial-temporal variations of the magnetic and gravitational field and relationship with the internal structure and dynamics of the earth's crust, volcanic and geothermal phenomena, erosion processes, etc. The most important source of information will be radar images at frequencies $<$ 1 GHz, making it possible to avoid the influence of the vegetation cover, and also the techniques of highly precise radioaltimetry.

The objective of the oceanological research section includes obtaining global information on the ocean at an almost real time scale, including information on temperature and the state of the ocean surface, salinity, currents, global circulation, tides, tsunamis, parameters of interaction between the ocean and the atmosphere, ice conditions, shore processes, etc. (a considerable part of this information has very great importance for the climate problem).

In order to obtain the mentioned information it is proposed, in particular, that on the orbital station "Spacelab" there by testing of a radar with a synthesized aperture satisfying the following requirements: preliminary processing of data on board, variable scanning band (10-500 km), variable resolution (5-50 m), multichannel capability (1-20 GHz), measurements in two polarizations. At the same time, use will be made of scatterometers, multiwave radiometers, laser apparatus and radioaltimeters. For example, using data from microwave radiometry it is possible to determine: salinity variations (at a frequency of 1.4 GHz), temperature of the ocean surface (6 GHz), degree of coverage with foam - wind velocity (10 GHz). The sensing of plankton, bottom sediments and contaminants of the ocean surface is possible using data in the optical range.

The development of a multichannel scanning microwave system, intended for measurements of radiothermal radiation of the underlying surface and the atmosphere, and also obtaining corresponding images [11], is of particular importance from the point of view of monitoring of climate; this is to be done within the framework of preparations in the scientific program for the shuttle. At the same time, use should be made of instrumentation for obtaining images in the visible and infrared spectral regions. The launchings of the shuttles planned for the beginning of the 1980's will afford still broader prospects for the use of the methods for microwave remote sensing. A factor of particularly great importance is a relaxation of weight restrictions and the related possibility of using large antennas, which will make possible a considerable increase in the spatial resolution of microwave systems and the use of radiometers operating at longer wavelengths than before (plans call for the broadening of the range in the direction of shorter wavelengths).

Two types of experiments are being prepared: 1) measurements of the radiothermal radiation of the atmosphere near the limb of the planetary disk at short wavelengths for the purpose of remote sensing of the upper layers of the atmosphere; 2) remote sensing of the parameters of the underlying surface and the atmosphere using measurements of the radiothermal radiation of the "earth's surface - atmosphere" system. Table 1 gives the set of wavelengths for the multichannel scanning microwave system to be used in solving problems in the second category. It should be noted here that in order to determine any of the parameters mentioned in the table it is necessary to have data on radiothermal radiation for the set of wavelengths.

Earlier experience has made it possible to evaluate the accuracy in determining some parameters. For example, the error in ascertaining the total water vapor content is about 0.2 g/cm^2, and of liquid water -- 0.01 g/cm^2. Zones of precipitation and the boundaries of the ice cover are reliably identified. In determining the water vapor content and the intensity of precipitation use will be made of the channels of the multichannel scanning microwave system operating at wavelengths 1.5, 1.3 and 0.9 cm, ensuring a spatial resolution of $\sim$3 km. Such a high resolution will make it possible, in particular, to trace the spatial-temporal dynamics of water vapor in hurricanes and in regions of lakes, which was impossible earlier.

The data for the channel 0.32 cm will make it possible to determine the position of the edges of sea and lake ice with a resolution of about 0.5 km. Simultaneous data for the channels 0.57 and 0.26 cm are very valuable from the point of view of mapping of storm conditions over the land. Preliminary estimates show that it is possible to attain an accuracy in determining temperature of the sea surface and wind velocity at the surface of about 1-2 K and 2 m/sec.

Data from aircraft measurements indicate that the accuracy in determining moisture content of the upper 15-cm ground layer (expressed in % by weight) is about 5% in the moisture content range 10-40%. In zones of very dry ground the thickness of the layer responsible for the formation of radiation is about 10 wavelengths. Therefore, in such cases the use of measurement data at long waves makes it possible to study subsurface phenomena at depths to several meters.

The multichannel scanning microwave system has no channels intended for sounding the atmosphere because the spatial resolution of this sytem is too high for such purposes. However, data for the channels 0.57 and 0.26 cm will nevertheless contain useful information on mean atmospheric temperatures.

A unique part of the multichannel scanning microwave system is a parabolic toroidal antenna whose diameter ($\sim$4 m) is dictated by the dimensions of the shuttle. An antenna of such a size ensures the necessary spatial resolution for all channels other than the three microwave channels, with scanning in the range 120° (virtually from horizon to horizon, in the direction perpendicular to the shuttle orbit). The scanning is accomplished by means of rotation of a flywheel to which radiometers are attached; this makes it possible to register radiation incident on the antenna from different directions. In order to ensure continuity of movement from one scanning line to the next (due to motion of the shuttle along the orbit) it is necessary that the velocity of rotation of the flywheel be $\sim$400 rpm. The stability of response of the multichannel scanning microwave system is monitored by means of on-board calibration using two radiation sources.

The successes associated with remote sensing of the atmosphere from space are based primarily on the development of passive sensing systems. An important contribution to the further improvement of these systems should come from introduction of the program for testing of new methods and instrumentation aboard the orbital station "Spacelab" [12]. The two approaches which have now been developed for solution of problems in the restoration of the vertical profiles of structural parameters and composition of the atmosphere were based on the use of measurements of the spectral intensity of outgoing radiation from the nadir zone or the atmospheric zone at the limb of the planetary disk. The realization of these approaches ensures the following typical spatial resolution in vertical and horizontal directions:

	Vertical resolution, km	Horizontal resolution, km
Nadir	10	25
Limb	2	200

The use of the methods of absorption or emission spectroscopy applicable to a "limb" model dominates in solution of problems of restoration of the concentration of small components in the stratosphere. The principal advantages in this case are exclusion of the influence of cloud cover and the possibility of measurement of quite large intensities of radiation or absorption by small components due to extended sighting paths.

In order to evaluate anthropogenic effects on the ozone layer, high-response instrumentation is being developed for the "Spacelab" orbital spacecraft. This will make it possible to determine the ozone content with a spatial resolution at the level of the earth's surface equal to 2 km [13]. The radiation receiver in the ozone detector installed in the focus of a 50.8-cm telescope is a mercury-cadmium-tellurium photoresistor. Instrumentation is also being prepared for installation on a geostationary satellite and having 150 similar photoresistors, which in 3 hours will make it possible to scan a territory measuring 4,000 x 6,000 km with a spatial resolution greater than 10 km.

Table 1

Microwave Remote Sensing of Parameters of Underlying Surface and Atmosphere

Wavelength, cm	Parameters to be determined
50	Ground moisture content, subsurface
21	phenomena, ocean salinity
11	
4.6	Temperature of sea surface
2.8	Waves, heavy precipitation
1.5	Water vapor content in atmosphere,
1.3	medium and light precipitation,
0.9	cloud microstructure
0.57	Storms over land
0.32	Water-ice boundary
0.26	Storms over land

Analysis of the prospects for using the "Spacelab" orbital station for investigations of the atmosphere and underlying surface led to the choice of the following potential set of instruments: filter photometer and radiometer, spectrometer with diffraction grating, Fabry-Perot and Michelson interferometers, correlation radiometer (with selective modulation and modulation by pressure), microwave radiometers, polarimeter, albedometer, television apparatus.

The enumerated instruments can be used in solving a great number of problems in remote sensing associated with study of dust aerosol and cloud cover in the troposphere, small components of the stratosphere, aerosol in the stratosphere (Junge layer) and the mesosphere (noctilucent clouds), neutral and ion composition of the mesosphere and thermosphere, for study of different components of aerosol and its contribution to the energy balance. An important place is occupied by the problem of restoration of the vertical temperature profile for the purpose of increasing restoration accuracy (to ±1 K) and using these data for an analysis of such phenomena as planetary waves, sudden heatings of the stratosphere and atmospheric tides.

The use of the Doppler method (employing Fabry-Perot standards, correlation spectrometers and microwave heterodyne radiometers) for restoration of the wind field is exceptionally timely and promising. Estimates show that it is possible to determine wind velocity in the troposphere and upper atmosphere with an accuracy of about ±3 and ±3-10 m/sec respectively (in the second case errors to ±30 m/sec can be considered acceptable).

The use of the Doppler method, assuming exclusion of the component of the Doppler shift of the spectral lines caused by the characteristic motion of the orbital station, involves rather rigorous requirements on the accuracy in determining the spatial orientation of the orbital station (to ±0.025° with respect to pitching and yawing and ±0.003° with respect to banking).

Three atmospheric layers (0-15, 15-70 and 70-140 km) are discriminated when planning specific scientific programs. The following four modules are planned for corresponding groups of problems. The instrumentation of module A provides for the restoration of temperature: kinetic -- layer 70-120 km (microwave measurements in the oxygen line), 70-140μm (Fabry-Perot standard); rotational -- microwave radiation of oxygen (118 GHz), IR radiation of CO_2 (band 15 μ m); vibrational -- microwave radiation of oxygen (118 GHz), IR radiation of CO_2 (bands 4.3 and 15μm).

The sources of information on composition of the atmosphere are: luminescence of atomic oxygen (130.4; 557.7; 630.0 nm); radiation in the far-IR region (63 and 147μm); microwave radiation of ozone (184 GHz); IR fluorescence and microwave radiation of CO (115 or 230 GHz) and H_2O (183 GHz), as well as measurements of the most important emissions: hydroxyl -- in the near-IR region, atomic oxygen (see above), molecular oxygen ($^1\Delta$ bands in the interval 1-27μm and $^1\Sigma$ at 700μm).

The principal purpose of the B module is restoration of the temperature profile (using data for the 15-μm band) and the aerosol concentration and also the following small gas components: H_2O, CO, CH_4, NO, NO_2, HNO_3, N_2O, HCl, HF, ClO, CH_2, chlorfluoromethanes, SO_2 and others. The central purpose of module C is restoration of the temperature field (data for the IR and the microwave region of the spectrum, hypothetically -- UV and visible radiation) and restoration of the wind field (IR and microwave, UV and visible spectral regions). The program for module D is spectropolarization measurements in the interval 0.4-2.2μm for the purpose of restoring the characteristics of clouds and aerosol. In almost all cases a "limb" measurement scheme is provided for.

A discussion of the prospects for using satellite active radar, carried out in July 1974 under the aegis of NASA, led to the conclusion that it is possible to solve a variety of problems in remote sensing of the atmosphere [14]. Satellite meteorological radar at a wavelength of 0.86 cm will make it possible to obtain information on the three-dimensional fields of some meteorological parameters in zones of tropical storms and monitor the evolution of storms with time. In particular, mapping of the altitudes of maximim echoes from rain will afford a possibility for characterizing the intensity of storms and precipitation. The possibility of restoring the altitude of the zero isotherm in rain clouds (it is usually situated approximately 200 m above the peak of the bright zone) is of great importance from the point of view of use of this type of data in numerical weather forecasts and in evaluating the intensity of tropical storms. The global mapping of precipitation intensity is of great interest for climatology.

The use of radar data for different wavelengths and polarizations will make it possible to solve problems in the restoration of water content and the microstructure of clouds. An experiment carried out on the "Skylab" orbital station demonstrated the practical possibility of using active radar for estimating wind velocity and direction at the ocean surface. The mapping of sea ice is a completely refined sphere of radar application.

The use of a multiwave radar operating in the oxygen band (0.5 cm) will afford important possibilities for solving the problem of restoration of atmospheric pressure at sea level (the minimum requirements provide for measurements at frequencies of 51 and 52.5 GHz). It is evidently possible to use multiwave radars for detecting cirrus clouds, differences in water and ice clouds, rain and snow. A Doppler radar operating at a wavelength of 5.6 cm can be employed in estimating the mean wind velocity in rain clouds with the use of precipitation particles as tracers of atmospheric movements.

The successful testing of different methods for microwave remote sensing of environmental parameters has encouraged NASA to accelerate further development in this field. As already noted, microwave systems are an important component of programs for the "Seasat" oceanographic satellites and reusable transport ships. In this connection J. W. Rouse [15] has deemed promising the development of methods for microwave remote sensing during the

course of the next 10 years; special attention was devoted to the development of active radar for the purpose of obtaining images of the earth's surface.

The first stage in the considered work is the preparation of a radar for obtaining images (ROI); it is planned that this be installed in transport ships in 1979, having in mind, in particular, a determination of soil moisture content. The ROI functions at a frequency of 1275 MHz, ensuring a resolution of $\sim$ 40 m with a width of the scanning band equal to 50 km, which is situated at an angle of 50° relative to the vertical. A modified variant of the radar for obtaining images (ROIM) is being developed for the "Spacelab" orbital station. Plans call for the use of this instrument for approximately 5 years, beginning in 1982-1983. The ROIM is a three-channel apparatus (ranges X and C or L). The synthesized apparature of this radar ensures a resolution of 25 m with a width of the scanning band 25 km. In two channels the ROIM operates with an identical horizontal polarization; the third channel in the X band also ensures measurements with vertical polarization. The deployable radar antenna has a length > 10 m and a width of 5 m, ensuring the obtaining of images of the underlying surface in the range of nadir angles 10-60°. The ROIM is fully supplied with a digital data processing system.

Table 2 gives the comparative characteristics of ROI and ROIM parameters. In the case of the "Climsat" satellite the deployable ROI (L range) is intended for determining soil moisture content with a spatial resolution 10-15 km for a nadir angle of 30°. The main objective of the promising developments associated with use of the active radar method is supplementation of the observational capabilities of the "Landsat" natural resources satellites with a capability for all-weather remote sensing of the characteristics of natural features.

Table 3 illustrates the comparative capabilities of the multichannel scanning instrumentation (MSI) on the "Landsat" satellites and active radar methods (ARM). The great promise of ARM determines the feasibility of including radars in the complex of scientific instrumentation on the "Landsat-E" or "Landsat-F" satellites. This will require serious efforts for the purpose of creating methods for the processing of data, and, in particular, an onboard system for processing the collected information.

The development of a reusable transport ship will make it possible to have a convenient platform for remote measurements of global aerosol on the basis of use of laser sounding methods from a transport ship. In this connection a review has been made of the present status of investigations of aerosol of the deserts and the characteristics of atmospheric molecular absorption [16]. The particular attention to desert aerosols is determined by its global propagation and its great contribution to the absorption of solar radiation by the atmosphere. The deserts, constituting $\sim$8% of the earth and $\sim$ 1/3 of the land surface, are the most powerful source of global aerosol.

Table 2

Comparative Characteristics of ROI and ROIM Parameters

Parameter	ROI	ROIM	
Range	L	X	C
Frequency, MHz	1275	9660	5380
Nominal altitude, km	200	225	225
Band width, km	5	10-15	10-15
Pulse power, KW	0.3	50	1.5
Polarization	hor	hor-ver	hor
Spatial resolution, m	6 x 40	4.5 x 25	4.5 x 25
Width of scanning band, km	59	25-50	25-50
Noise level, db	-37	-38 at 47°	-41 at 47°

On the assumption that in numerical modeling of general circulation of the atmosphere errors in determining radiation measurements of temperature not exceeding 0.2 or 0.5 degree/day are not significant, in [16] the authors evaluated the requirements on data from remote laser sensing of aerosol from a transport ship. It is demonstrated that the present-day level of instrument development makes it possible to satisfy the second of the mentioned accuracy criteria, whereas the first can be satisfied with the continuing improvement of the lidar soundings method up to the time of functioning of the transport ships. Source [16] gives the results of computations characterizing the possible errors in determining the aerosol attenuation coefficient at different altitudes using laser sounding data at a wavelength of 0.5μm. These evaluations were obtained for the conditions of a "normal" dust content in the atmosphere (the mass concentration of aerosol is equal to 300$\mu g/m^3$ and in this case was adopted as unity: BF = 1, and also BF = 0, 0.1, 5 and 10). The cases BF = 1 and BF = 5 correspond closely to models of a pure and dust-filled tropical atmosphere. A horizontal range of visibility at the earth's surface of 22 and 4.5 km corresponds to these models.

Evaluations show that restoration of the vertical profile of the aerosol attenuation coefficient with a vertical resolution of remote sensing of 1 km does not lead to errors in determining radiation changes in temperature for individual layers of the atmosphere exceeding 0.2 degree/day. The absolute maximum error is a total of 0.055 degree/day. Thus, a resolution of 1 km is entirely acceptable.

The importance of taking into account the influence of solar-terrestrial relationships on the environment determines the necessity for examining the unified sun-earth system and carrying out a set of observations, including the sun and circumterrestrial space. The good possibilities for shuttle transport ships and "Spacelab" orbital stations are affording possibilities for carrying out a multisided program for investigations of the sun, upper and lower layers of the atmosphere, which is necessary for understanding the physical nature of solar-terrestrial relationships. The complexity of such a program and the need to regulate its implementation depending on developing conditions (such as the appearance of a solar

Table 3

Comparative Possibilities of Multichannel Scanning Apparatus and Active Radar Methods

Interpretation region	Instrumentation		
	MSA	ARM	MSA + ARM
Soil moisture content	Soil color	Evaluation of soil moisture content	Maps of soil moisture content
Identification of agricultural crops	Vegetation spectra	Moisture reserve for plants Morphology of vegetation cover	All-weather identification of agricultural crops
Geological structures	Vegetation distribution	Surface images through vegetation cover	Refinement of geological maps
Snow cover	Albedo, distribution of snow cover	Type and thickness of snow cover	All-weather information on snow cover
State of surface	Color of surface Distribution of vegetation	Roughness Surface composition	Refinement of maps of surface characteristics
Biomass	Distribution of vegetation Estimate of biomass	Soil moisture content	Influence of soil moisture content on biomass

flare, etc.) determine the choice of manned orbital stations as the most suitable research tool [17]. The creation of a manned orbital solar-terrestrial observatory should be the long-range objective.

The first step on the path to such an observatory should be the use of low-orbit transport ships and the "Spacelab" orbital station. In the future it will be very important of have observations from a geosynchronous orbit, making it possible to achieve the necessary spatial integration in the study of such phenomena as auroras, night air glow, etc. C. R. Chappell [17] described a program for developing methods for space monitoring in the interests of the problem of solar-terrestrial relationships.

The program for observations of the sun provides for the use of such apparatus as an optical telescope with a diameter of 1 m, spectroheliographs for the x-radiation and hard UV ranges, coronagraphs for study of the solar corona in the visible region of the spectrum in the Lyman-alpha line. An extensive complex of instrumentation is being prepared for investigations of the magnetosphere with the use of three methods: 1) remote sensing of magnetospheric parameters; 2) active modification of the magnetosphere with monitoring of its effects by means of direct and remote measurements; 3) passive observations of magnetospheric plasma.

For such artificial modification plans call for the injection of waves, ionized gases and beams of particles, having in mind the simulation, under real conditions, of the processes which can transpire in the magnetosphere. It is proposed that at the same time there be measurements of the solar wind from automatic satellites.

Passive measurements of the characteristics of magnetospheric plasma also can be made from automatic artificial earth satellites. In order to make remote determinations of atmospheric parameters it is possible to use a method for obtaining images in different parts of the spectrum (observations of the spatial-temporal structure of auroras and nightglow), and also passive and active (lidar) remote sensing. Measurements on slant paths in the atmospheric zone at the horizon, making it possible to restore vertical profiles of upper atmosphere characteristics, are most promising.

The already adopted observation program provides for the use of the first two flights of the "Spacelab" orbital station and includes: measurements of the integral and spectral solar constant, solar magnetic field; experiments with modification of the magnetosphere by streams of particles. An extensive complex of technical units constitutes the instrumentation for remote sensing: instruments for scanning the limb for the purpose of restoring the composition of the atmosphere; interferometers for measuring temperature and wind; imaging apparatus making it possible to investigate auroras. An important characteristic of the described program is its development on the principles of international scientific cooperation.

BIBLIOGRAPHY

1. Bugayev, V. A., Popova, T. P., Yakovleva, T. P., "Meteorological Observations on the Orbital Station 'Salyut'," METEOROL. I GIDROLOG. (Meteorology and Hydrology), No 4, pp 8-13, 1974.

2. Kondrat'yev, K. Ya., "Meteorological Investigations on Manned Spaceships (Review)," IZV. AN SSSR, FIZIKA ATMOSF. I OKEANA (News of the USSR Academy of Sciences, Physics of the Atmosphere and Ocean), Vol 2, No 7, pp 740-757, 1966.

3. ISSLEDOVANIYA PRIRODNOY SREDY S PILOTIRUYEMYKH ORBITAL'NYKH STANTSIY (Investigations of the Environment from Manned Orbital Stations), edited by K. Ya. Kondrat'yev, Leningrad, Gidrometeoizdat, 1972.

4. Kondrat'yev, K. Ya., Buznikov, A. A., Pokrovskiy, O. M., "Determination of Vertical Aerosol Profiles in the Atmosphere According to Results of Spectrophotometric Measurements of the Earth's Total Horizon from the 'Soyuz-13' Spaceship," DOKL. AN SSSR (Reports of the USSR Academy of Sciences), Vol 235, No 1, pp 53-56, 1977.

5. Kondrat'yev, K. Ya., Buznikov, A. A., Pokrovskiy, A. G., "Determination of Small Gas Components in the Stratosphere by the Eclipse Sounding Method," IZV. AN SSSR, FIZIKA ATMOSF. I OKEANA, Vol 14, No 12, pp 1235-1248, 1978.

6. Lazarev, A. I., Nikolayev, A. G., "Results and Prospects of Optical Investigations of the Earth's Upper Atmosphere from Space," TR. IN-TA EKSPERIM. METEOROL. (Transactions of the Institute of Experimental Meteorology), No 8(81), pp 109-130, 1978.

7. Shatalov, V. A., Sandomirskiy, A. B., Sergeyevich, V. N., Stol'berg, B. M., "Determination of the Vertical and Energy Scales for a Photometric Analysis of Photographs of the Earth's Atmospheric Aureole from Space," KOSMICH. ISSLEDOVANIYA (Space Research), Vol 13, No 6, pp 907-913, 1975.

8. Nikolayev, A. G., Sevast'yanov, V. I., Sandomirskiy, A. V., Stol'berg, V. M., "Determination of Altitude of the Earth's Optical Horizon from the 'Soyuz-9' Spaceship," KOSMICH. ISSLEDOVANIYA, Vol XIV, No 3, pp 467-469, 1976.

9. Sevast'yanov, V. I., "Some Results of Implementation of the Scientific Research Program During the Prolonged Spaceflight of the 'Salyut-4,'" TR. DESYATYKH CHTENIY, POSVYASHCHEN. RAZRAB. NAUCHN. ISSLED I RAZVITIYU IDEY K. E. TSIOLKOVSKOGO (Transactions of the Tenth Readings Devoted to Development of Scientific Research and the Development of the Ideas of K. E. Tsiolkovskiy), Kaluga, 16-19 Sep 1975), Moscow, pp 9-13, 1977.

10. Durrani, S., Golden, T., Morakis, J., Waetjen R., Deskevich, J., "Potential Shuttle Spacelab Applications," NASA X-950-74-70, Goddard Space Flight Center, 1974, 64 pages.

11. Waters, J. W., Barath, F. T., Chow, E. Y., Goetz, A. F. H., Johnston, E. J., Stacey, J. M., Gustincic, J. J., Staelin, D. H., Kong, J. A., Njoku, E. G., Kunzik, K. F., Muhleman, D. O., Wilheit, T. T., "The Shuttle Imaging Microwave Experiment," PREPRINT IEEE 1975 National Telecomm. Conf., Vol 11, New Orleans, Dec 1-3, 1975, 5 pp.

12. Harries, J. E., "The Role of Passive Sounder Packages on Spacelab," ATMOSPHERIC PHYSICS FROM SPACELAB, D. Reidel Publ. Co., Dordrecht, Holland, pp 265-276, 1976.

13. Lovill, J. E., Sullivan, T. J., "An Extremely High-Resolution Ozone Sensor for Spacelab," PROC. JOINT SYMP. ATMOS. OZONE, Dresden, 1976, Vol 1, Berlin, 1977, p 201.

14. Katz, I., "Active Microwave Sensing of the Atmosphere from Satellites," 16th RADAR METEOROL. CONF., Houston, Tex, 1975, Boston, Mass, pp 246-252, 1977.

15. Rouse, J. W., Jr., "Predictions on Future Use of Active Microwave Systems for All-Weather Sensing of the Earth," AIAA PAP., No 1584, pp 1-6, 1977.

16. Shipley, S. T., Joseph, J. H., Trauger, J. T., Guetter, P. J., Eloranta, E. W., Lawler, J. E., Wiscombe, W. J., Odell, A. P., Roester, F. L., Weinman, J. A., "The Evaluation of a Lidar Experiment to Obtain Meteorological and Air Quality Measurements from a Space Shuttle Platform," FINAL REPORT ON NASA Grant NSG-1057, Dept. of Meteorology, Univ. of Wisconsin, Madison, Wisconsin, April 1975, 60 pages.

17. Chappell, C. R., "The Solar Terrestrial Observatory," AIAA PAPER, No 80, 1978.

[352-5303]

5303
CSO: 1866

- END -

APPROVED FOR RELEASE: 2007/02/08: CIA-RDP82-00850R000300030023-0